People`s Democratic Republic of Algeria
Ministry of Higher Education and Scientific Research
University of EchahidHammaLakhdar - El Oued
Faculty of Technology
Department of mechanical engineering

ACADEMIC MASTER

Domain: Science and Technology

Division: Electromechanical

Specialty: Electromechanical

Presented by:

1.TAGHIA Abdelbasset

2. MIM Ahmed

Entitled:

Sliding Mode Control of A Six Phase Induction Machine

Dissertation Submitted in Partial Fulfillment of the Requirements for the Master Degree in Faculty of Technology

Publicly defended in: 29/05 /2025

Board of Examiners:

Dr : MOHREM ABDELKARIM	**Chairman**
Dr : HAMZA MESAI AHMED	**Supervisor**
Dr : MAHMOUDI ABELKADER	**Examiner**

Academic Year: 2025/2024

Dedication

I dedicate this work

My dear parents in particular

to my brothersAnd my sisters

To Dr. Mesai Ahmed Hamzaand

For my whole family in general

To all my friends

Ahmed

Dedication

I dedicate this work to my father,

who is the result of long work and study, to my dear mother and father who has never been stingy with his advice, to my wife and life partner,

to my brothers, sisters, friends and extended family. I also dedicate it to my respected teachers, especially Dr. MessaiAhmed Hamza.

Abdelbasset

Remerciements

First, we thank God Almighty for granting us the strength and determination to complete this project.

We extend our sincere thanks to our supervisor, ***Dr. Massai Ahmed Hamza****, for his presence, his enthusiasm in proposing and following up on our project, and his valuable advice.*

I also extend my sincere thanks to all members of the judging committee for agreeing to judge this project.

List of figures:

SYMBOLS

- Modeling Parameters of 6PH-IM **:**

R_s	(Ω)	Stator resistance per phase,
R_r	(Ω)	Rotor resistance per phase,
L_s	(H)	Stator cyclic inductance by phase,
L_r	(H)	Rotor cyclic inductance per phase,
L_m	(H)	Mutual cyclic inductance (between stator and rotor), magnetizing inductance,
l_s	(H)	Specific inductance of a statoric phase,
l_r	(H)	Clean inductance of a rotor phase,
m_s	(H)	Mutual inductance between two stator phases,
m_r	(H)	Mutual inductance between two rotor phases,
M	(H)	Maximum value of mutual inductance between stator phase and other rotoric phase,
p	(–)	number of pole pairs,
C_{em}	(N.m)	Electromagnetic torque of the generator

- **Repere :**

(s_a, s_b, s_c)	Magnetic axes linked to three-phase stator windings,
(r_a, r_b, r_c)	Magnetic axes linked to three-phase rotor windings,
(dq_1), (dq_2)	Park reference axes,
($\alpha\beta_1$), ($\alpha\beta_2$)	Concordia/Clarke reference axes,
θ_{sr} (rad)	Rotor angular position relative to stator,
θ_s (rad)	Stator angular position relative to axis (d).
θ_r (rad)	Rotor angular position relative to axis (d).

- Electrical quantities**:**

$v_{s\,abc1}$, $v_{s\,abc2}$	(V)	Three Phase Instantaneous Stator Voltages,
$v_{r\,a,\,b,\,c}$	(V)	Three Phase Instantaneous Stator Voltages,
$v_{s\,dq1}$, $v_{s\,dq2}$	(V)	Two-phase stator voltages in landmark (d, q),
v_{rdq}	(V)	Two-phase stator voltages in landmark (d, q),
V_s	(V)	Stator Voltage Vector Module,
$i_{s\,abc1}$, $i_{s\,abc2}$	(A)	Three Phase Stator Instantaneous Currents,
i_{rabc}	(A)	Three Phase Stator Instantaneous Currents,
$i_{s\,dq1}$,$i_{s\,dq2}$	(A)	Two-phase stator currents in landmark (d, q),

i_{rdq}	(A)	Two-phase stator currents in landmark (d, q),
$\phi_{s\,abc1}, \phi_{s\,abc2}$	(Wb)	Instant Magnetic Flow to Stator,
$\phi_{s\,dq1}$, $\phi_{s\,dq2}$	(Wb)	Two-phase stator flows in the rotating landmark (d, q).
Ψ_s	(Wb)	Stator flux vector module.
$\phi_{rab\,c}$	(Wb)	Rotor magnetic flux vector,
ϕ_{rdq}	(Wb)	Two-phase rotor flows in the rotating landmark (d, q).
Ψ_r	(Wb)	Rotor Flux Vector Module.
P_s	(W)	Stator Active Power,
Q_s	(VAr)	Stator reactive power.
$P_{réseau}$	(W)	Power supplied to the network,

- Mechanical quantities **:**

ω_r	(rad/s)	Electric pulse corresponding to the speed of rotation,
ω_s	(rad/s)	Electric pulsation of stator quantities (rotating field),
G	(–)	Rotation speed shift,
f_s	(Hz)	Electrical frequency of stator quantities,
f_r	(Hz)	Electrical frequency of rotor quantities,
N_s	(tr/min)	Speed of the rotating field,

- **Transformations :**

s	Laplace operator,
$P(\theta)$	Park Transformation:$X_{sa,b,c} \rightarrow X_{sd,q}etX_{ra,b,c} \rightarrow X_{rd,q}$,

- Control quantities of the 6PH-IM **:**

K_p, K_i	(–)	Proportional and integral components of the PI corrector,
r	(–)	Modulation rate (adjustment index),
m	(–)	modulation index,
f_r	(Hz)	reference frequency,
w_i	(–)	Weight vector
η_i	(–)	learning rate
ψ_i,ϕ_i,	(–)	vector-valued functions
P_i	(–)	Predicate error
H_i	(–)	Matrix gradient
Q_i, R_i	(–)	matrices de covariance
S	(–)	Fonction de limite

α, β	(–)	Constant values

NOTATIONS

6PH-IM	: Six phase induction machine.
MSC	: Machine Side Converter.
CVI	:Indirect Vector Control.
MCC	: Machine à Courant Continu.
PWM	: Pulse Width Modulation.
PI	: Proportional Integral.

AC	: Alternatif Current.
DC	: Direct Current.
FOC	: Field Oriented Control.
ANN	: Artificial Neural Networks.
RNN	: Recurrent Neural Networks.
EKF	: Extended KalmanFilter .
MPC	: Model Predictive Control
PCC	: Predictive Current Control
MB-PCC	: Model-Based Predictive Current Control
MF-PCC	: Model-Free Predictive Current Control
MPPT	: Maximum Power Point Tracking.
MLP	: Multi Layer Perceptron.
IGBT	: Insulated Gate Bipolar Transistor.
NPC	: Neutral Point Clamped.
WECS	: Wind Energy Conversion Systems.

Abstract:

In recent years, Multiphase machines are increasingly used in high power applications forreasons of reliability and power segmentation. The six-phase induction machine (6PH-IM)was one of such machines. It consists of two sets of identical three-phase windings in thesame stator, and supplied by two voltage converters. Several researches are currentlydirected towards the applications of advanced control algorithms to improve theperformance of the machine . This thesis aims to study by simulation the sliding modecontrol (SMC) of a six-phase induction machine driven by two voltage converters.

Key words:

Multiphase machines, Six phases induction machine (6PH-IM), Sliding mode control(SMC), Power converters.

Résumé:

Ces dernières années, les machines multiphasées sont de plus en plus utilisées dans lesapplications de forte puissance pour des raisons de fiabilité et de segmentation depuissance. La machine à induction 6 phases (6PH-IM) en fait partie. Elle est constituée dedeux jeux d'enroulements triphasés identiques dans le même stator et alimentée par deuxconvertisseurs de tension. Plusieurs recherches portent actuellement sur l'applicationd'algorithmes de contrôle avancés pour améliorer les performances de la machine. Cettethèse vise à étudier par simulation la commande par mode glissant (SMC) d'une machine àinduction 6 phases pilotée par deux convertisseurs de tension.

Mots clés :

Machines multiphases, Machine asynchrone à six phases (6PH-IM), Commande à modeglissant (SMC), Convertisseurs de puissance.

الملخص:

في السنوات الأخيرة، ازداد استخدام الآلات متعددة الأطوار في تطبيقات الطاقة العالية لأسباب تتعلق بالموثوقية وتجزئة الطاقة. وكانت آلة الحث سداسية الأطوار (PH-IM6) إحدى هذه الآلات. تتكون من مجموعتين متطابقتين من اللفات ثلاثية الأطوار في الجزء الثابت نفسه، ويتم تزويدها بالطاقة بواسطة محولي جهد. وتُجرى حاليًا العديد من الأبحاث حول تطبيقات خوارزميات التحكم المتقدمة لتحسين أداء هذه الآلة. تهدف هذه الرسالة إلى دراسة محاكاة التحكم في وضع الانزلاق (SMC) لألة حث سداسية الأطوار تعمل بواسطة محولي جهد.

كلمات مفتاحية :

آلات متعددة الأطوار, آلة حث الأطوار, التحكم في وضع الانزلاق, محولات طاقة.

General Introduction

General Introduction

In the evolving landscape of electrical drive systems, the demand for higher power density, fault tolerance, and increased reliability has led to a growing interest in multiphase machines. Among these, the six-phase induction machine (6PH-IM) has emerged as a strong candidate for applications in electric vehicles, renewable energy systems, ship propulsion, and industrial automation. Its inherent advantages, such as improved torque density, lower current per phase, and enhanced fault tolerance compared to traditional three-phase machines, make it a suitable solution for high-performance and safety-critical applications.

Despite these advantages, the control of six-phase induction machines presents unique challenges due to their increased complexity, multi-dimensional current and flux dynamics, and interaction between multiple subspaces. In this context, advanced control strategies become essential to exploit the full potential of these machines. One of the most promising methods in this regard is **Sliding Mode Control (SMC)** — a nonlinear control technique known for its robustness to parameter variations and external disturbances, as well as its ability to ensure fast dynamic response and precise tracking.

This dissertation is dedicated to the study and application of Sliding Mode Control for the six-phase induction machine. The aim is to model the machine accurately and implement a robust control strategy that enhances its dynamic performance under various operating conditions.

The work is structured as follows:

- **Chapter 1: Multiphase Machines – Overview, Challenges, and Context of Study**
  This chapter provides a comprehensive overview of multiphase machines, focusing on their advantages over conventional three-phase systems, their practical applications, and the specific challenges they pose. It also positions the six-phase induction machine within this broader context and justifies the choice of control strategy.
- **Chapter 2: Study and Modeling of the Six-Phase Induction Machine**
  This chapter details the theoretical modeling of the 6PH-IM, including its electrical and mechanical equations. Both the α–β and d–q modeling approaches are considered, with a

focus on the decoupling of the two three-phase subspaces. The chapter concludes with the simulation setup and validation of the machine model.

- **Chapter 3: Sliding Mode Control of the Six-Phase Induction Machine**
  In this chapter, the Sliding Mode Control strategy is developed and applied to the machine model. The design of the sliding surfaces, the control law, and methods for chattering reduction are discussed. Simulation results are presented to evaluate the performance of the SMC under different load and disturbance scenarios, and are compared to conventional control methods.

This dissertation aims to demonstrate the viability and advantages of using Sliding Mode Control in the context of six-phase induction machines and to contribute to the ongoing research in multiphase drive systems.

Chapter I

Multiphase systems: state of the art, problematic and work context

I.1 Introduction:

Induction motors remain one of the most widely used types of electric motors in industrial applications, maintaining their popularity for over a century. Their durability, cost-effectiveness, and low maintenance requirements make them a preferred choice over DC motors and other AC motors. In recent years, increasing attention has been given to multiphase induction motors, where the number of stator phases exceeds three. These motors offer several advantages in terms of performance, reliability, and efficiency, making them suitable for various advanced applications.

This chapter provides an overview of the history of electrical machines, followed by a definition of multiphase motors and an explanation of their working principles and characteristics. Additionally, their advantages and disadvantages in different applications will be discussed. Finally, a general overview of control strategies applied to six-phase induction machines will be presented.

I.2 General information on the machines:

I.2.1 History of electric machines:

The development of electric machines has evolved over two centuries, beginning with the foundational work on electromagnetism in the early 19th century. Michael Faraday's discovery of electromagnetic induction in 1831 marked a pivotal moment, enabling the transformation of mechanical energy into electrical energy and vice versa. This principle laid the groundwork for both electric generators and motors. In the late 1800s, Nikola Tesla and Thomas Edison contributed significantly to the commercial development of electric power systems, with Tesla’s invention of the alternating current (AC) motor playing a key role in modern energy distribution. The 20th century witnessed rapid advancements in electric machine design, efficiency, and control, particularly with the rise of power electronics and digital control systems. Today, electric machines are indispensable in industrial automation, transportation, renewable energy, and consumer electronics, continuing to evolve with trends in smart grids, electric vehicles, and high-efficiency drives.

Since the end of the 1920s, machines with two three-phase stator windings had been introduced to increase the power of very high-power synchronous alternators[MESS18].

I.2.2 Classification of electrical machines

The classification of machines can be done in several ways:

- According to the way of supplying or delivering the current/voltage.
- According to the construction.

I.2.3 Depending on the type of current

- Direct Current Machines.
- DC machines either series, parallel or compound.
- Alternating current machines.
- Synchronous machines.

I.2.4 Synchronous machines.

According to their construction.

- Asynchronous machines.
- Machines without collector.
- Permanent magnet synchronous machine.
- Machines with manifold.
- DC machines.

In addition, multiphase machines (whose number of phases is more than three) appeared in the years1920 for alternator power segmentation [BER16].

I.3 State of the art of multiphase induction machine:

I.3.1 Structuredesmachinesmulti phase:

We can classify the machines according to several ways either by its way of feeding (way of delivering the current/voltage) or by its construction. The machine can be asynchronous with wound rotor, with squirrel cage or synchronous with permanent magnets, with excitation windings, with smooth poles or with salient poles, with or without dampers. These machines can be powered by current switches or voltage inverters. Multi-phase machines, as its name suggests, behave like the classic three-phase asynchronous machine two parts[RAH20] :

- A rotating part with a solid cylindrical shape on a shaft is the rotor which is built from windings connected to themselves:
- A stationary part with a hollow cylindrical shape is the stator which comprises several three-phase windings, magnetically coupled orotherwise, and whose respective phases

are grouped into several stars. Each star is powered by its own static converter.

I.4 The characteristics of multi-phase machines:

According to the number of phases that we can have in the stator (the stator phases) which is or multiple name of three, we distinguish two types of type 1 multi-phase machines" are called "multi-phase machines " and "type 2 multi-phase machines". Moreover, one rarely considers the or the number of phases is an even number except if this one is a multiple of three [HAD01].

There can be several possible configurations in a machine with a given number of phases depending on the angular offset α between two adjacent coils. That is to say the offset between the stars. To be able to differentiate between the possible configurations, another term can be introduced: the number of equivalent phases, it is defined as follows:

$$npha = \frac{\pi}{a} \quad \text{(I.1)}$$

For example: 6phase induction machine (6phase) , with angular offset between the stars $a = \frac{\pi}{6}$ has characteristics different from those of a machine having the same number of phases but their stars are shifted by $a = \frac{\pi}{3}$

I.4.1 Type 1 multi-phase machines:

In this type of machine the number of stator phases is a multiple of three, they can be grouped into η star, three-phase [HAD01].

$$nph = 3\eta (\eta = 1,2,3\ldots.) \quad \text{(I.2)}$$

Taple.1: machines whose number of stator phases is a multiple of three"type1"

Number of phases (q)	**Phase equivalentn umber (qa)**	**Angular offset (a)**	**Schematic representation, position of the coils**
3	**3**	$\frac{\pi}{3}$	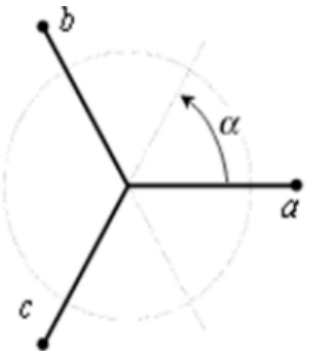
6	**3**	$\frac{\pi}{3}$	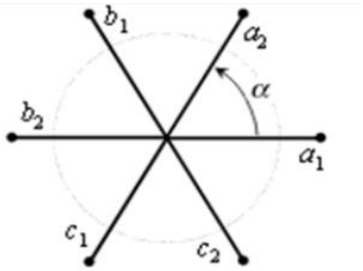
6	**6**	$\frac{\pi}{6}$	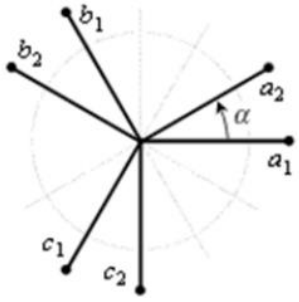

9	**9**	**$\frac{\pi}{9}$**	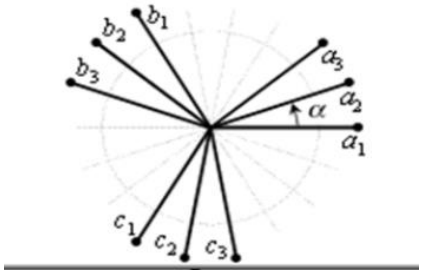
12	**6**	**$\frac{\pi}{6}$**	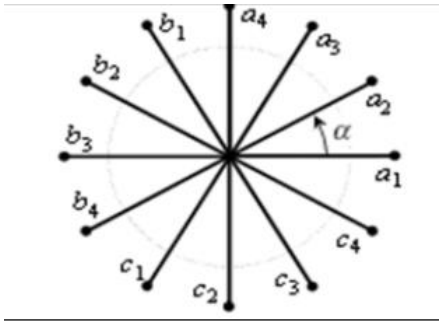
12	**12**	**$\frac{\pi}{12}$**	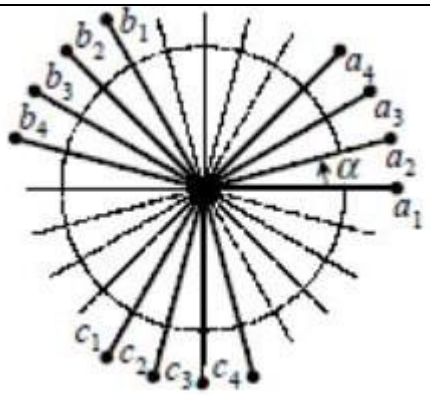

I.4.2 Type 2 multiple machines:

Type 2 multiple machines with an odd number of stator phases (nph).

$$nph=3\eta+1(\eta= 1,2,3\ldots.) \quad \text{(I.3)}$$

For the angular shift α between two adjacent coils, the phases of which are shifted regularly from $2a = \frac{2\pi}{nph}$ So we have $nph = nph_a = \frac{\pi}{a}$ (I.4)

Table.I.2: machines whose number of stator phases is an odd number ‘’type2’’.

Number of phases (q)	Phase equivalent number (qa)	Angular offset (a)	Schematic representation, position of the coils
5	5	$\frac{\pi}{5}$	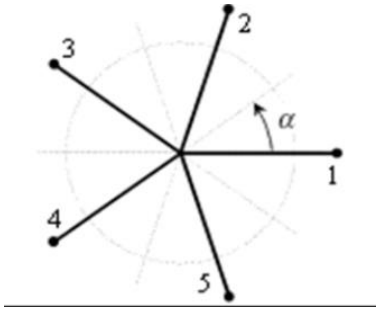
7	7	$\frac{\pi}{7}$	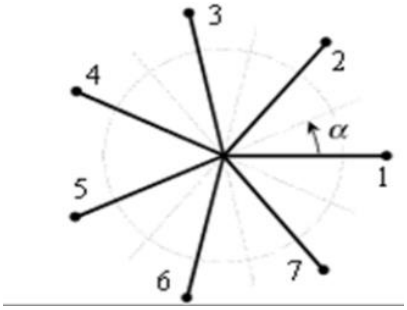
9	9	$\frac{\pi}{9}$	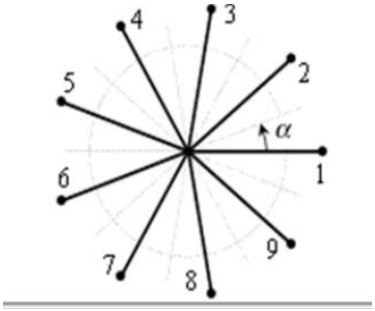

11	**11**	**π / 11**	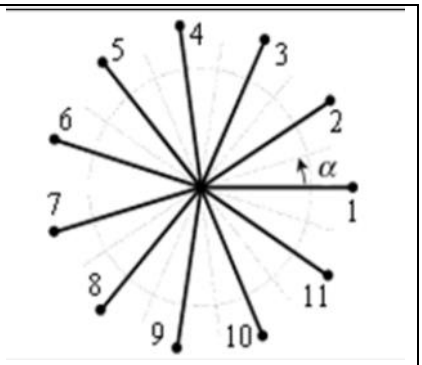
13	**13**	**π / 13**	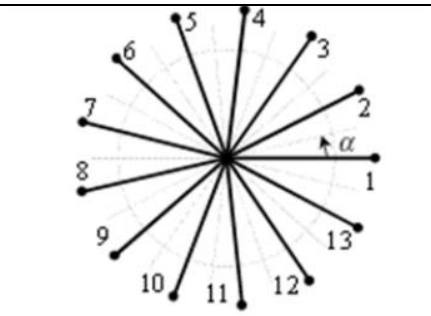

I.5 Operating principle of the multi-phase machine

- **Taking the six phase induction machine as an example**:

The stator currents create a rotating magnetic field in the two stators (star 1 powered by three-phase currents and star 2 powered by the same three-phase currents but shifted by an angle α). The rotational frequency of this field is imposed by the frequency of the stator currents, i.e. its rotational speed is proportional to the frequency of the electrical power supply, the speed of this rotating field is called synchronism speed. It defines as follows[RAZ00].

$w_s = \frac{t_s}{p}[rad/s]$(I.5)

These two rotating fields produced by the two stator windings will induce currents in the conductors of the rotor. Thus generating emfs that will cause the rotor to spin at a speed ωr less than that of synchronism ($\omega r < \omega s$), thus the effects of stator induction on rotor induced currents manifest as the development of an electromagnetic force couple on the rotor such that the speed

difference is reduced. The speed difference between the rotor and the stator field is called relative speed :

$$\omega=\omega_s-\Omega \qquad \text{(I.6)}$$

We will then say that these two fields slip with respect to the rotor and we define this slip by the ratio:

$$g = \frac{W}{Ws} = \frac{Wg - Wr}{Ws!} \qquad \text{(I.7)}$$

The different operating modes depend on the value of the slip:

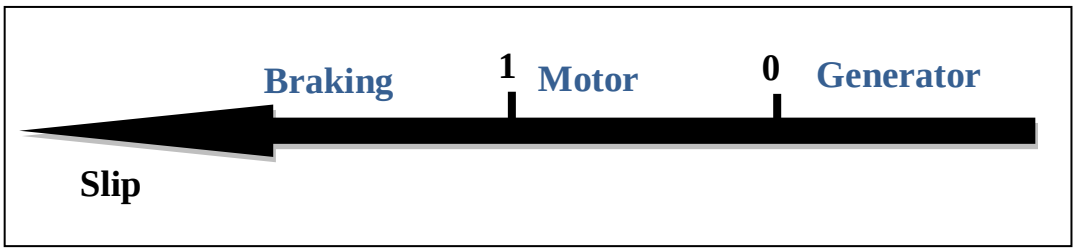

FigureI.1: Operating modes according to slip

I.5.1 Advantages of Multiphase Machines:

Many research studies on multi-phase machines have been conducted for reasons of reliability, power segmentation, and torque ripple minimization.

I.5.2. Power Segmentation

ncreasing the number of phases in an electrical machine leads to a rise in the overall system power, accompanied by an increase in the number of stator phases. As a result, the required power is distributed over a larger number of phases, thereby reducing the load on each individual phase.

Moubayed, N[Mou 99]explained that power segmentation in converter-machine systems represents an effective approach for supplying multi-star AC machines using multiple

independent voltage inverters. This strategy offers several advantages, most notably modularity at the inverter level, which enhances operational flexibility and ensures continued operation even under degraded or fault conditions.

In this context, synchronous and asynchronous double-star machines were modeled to be powered by two voltage inverters. Through analytical modeling, numerical simulation, and experimental validation, the study addressed the issues related to magnetic coupling between the stars, which may result in excessive currents within the phase windings.

The findings indicated that minimizing magnetic coupling between the stator stars, along with operating at the highest possible switching frequency, are essential factors for improving system performance. These conclusions were further generalized to apply to multi-star AC machines as a whole.

I.5.3. Reliability

The degraded operating mode (caused by the loss of one of the phases due to the failure of semiconductor components in the inverter supplying the machine) leads to a loss of machine control and high-amplitude torque ripples.

One solution to maintain control of the machine in this mode is to connect the neutral ofthe machine to the midpoint of the DC voltage source.

I.5.4. Minimization of Torque Ripple and Rotor Losses

Harmonics exist in a three-phase machine; however, in a double-star machine, they are naturally eliminated. It is observed that certain harmonics in the stator currents do not generate electromotive force (EMF), meaning that no induced currents appear in the rotor for these harmonics.As a result, a multi-phase machine will almost always have lower rotor losses compared to a three-phase machine Other advantages include improving the power factor and minimizing torque ripple and rotor losses[*OUA17*] .

I.5.5. Disadvantages of multi-phase machines:

However, the asynchronous machine has disadvantages such as [AMI08]

- ✓ The number of semiconductors increases with the number of phases, which may eventually increase the cost of the converter-machine assembly.
- ✓ The multiplication of the number of semiconductors with the dynamic structure is strongly nonlinear and the existence of a strong coupling between the torque and the flux, which obviously complicates its control.
- ✓ The major drawback of double star machines is the appearance of circulating harmonic currents when powered by a voltage inverter.

In our work we are interested in the six-phase machine

I.6 Six-phase "double star" machine models in the literature

The control of multi-phase machines is generally an extension of the control principles used for three-phase machines. As in the case of a three-phase machine, the control of a multi-phase machine is based on an appropriate machine model. In the particular case of a six-phase machine, two different models have been commonly used for the development of the control, namely the double-dq] model and the VSD model. For the double-dq model, two separate three-phase decoupling (Clarke) transformations are first applied to the two sets of energy and to the two sets of three-phase windings. Taking stator currents as an example, we get two pairs of α-β currents($i_1 i_1$and $i_2 i_2$) in the stationary frame. These currents are then subjected to a rotation transformation (Park), to give two pairs. corresponding d-q currents (i_{d1} i_{q1} et i_{d2} i_{q2}). Since the d axis is aligned with the rotor flux, the machine flux is controlled by regulating id1 and id2, while the machine torque is controlled by regulating iq1 and iq2. This is analogous to rotor flux-oriented control (RFOC) in three-phase machines, except that two sets of d-q current controllers are required instead of just one.

An implementation of current control based on this approach has been reported in An extension of this model to a nine-phase machine has been demonstrated in for an ultra-high-speed elevator application, using three decoupling transformations instead of two and three pairs of d-q current controllers. However, an obvious disadvantage of this model is that its application is limited to multiphase machines with several three-phase windings. An alternative to the double-dq model is the VSD model developed in[9]. The VSD model is an important tool for the analysis of polyphone machines and, subsequently, for the

development of current control methods. Using the VSD approach, an n-phase machine can be represented using n/2 (or (n-1)/2 for machines with an odd number of phases) orthogonal subspaces, innate an α-β subspace and several x-y subspaces, as well as the homopolar components. For a machine with a sinusoidal magneto motive force (MMF) distribution, only the α-β components contribute to the useful conversion of electromechanical energy, while the x-y and zero-sequence components only produce losses. Based on the VSD approach, the α-β equations of a polyphone machine are identical to those of a three-phase machine, so the direct implementation of standard three-phase vector control becomes possible. Nevertheless, due to the presence of additional loss-producing components, the corresponding currents must also be controlled to improve system performance. Compared to the double-dq model, the VSD model is more general and is applicable to polyphone machines of any number of phases. The separation of flux and torque producing components (α-β) from loss producing components (x-y and zero-sequence) in the VSD model provides an insightful tool for the development of spatial vector pulse width modulation (SVPWM) for multiphase machines, which cannot be done easily using the double-dq model. In terms of control, it was concluded that similar dynamic performance can be obtained regardless of the type of model chosen. Nevertheless, it has also been noted in that six-phase machine vector control using the VSD approach requires voltage decoupling terms that are less complicated than in the double-dq approach. It should be noted that although the VSD and double-dq models are essentially applicable to the same machine, the machine parameters for each model are different. In, it has been shown that if the mutual leakage inductance between the two three-phase windings is considered negligible, a simple and direct correlation between the parameters of the two models exists. The stator resistance and stator leakage inductance are equal for both models, while the mutual inductance, rotor leakage inductance and rotor resistance of the VSD model are twice that of the dual model -dq. Despite the various advantages of the VSD model, the variables are more difficult to physically interpret, unlike the double-dq model where dq1 is clearly tied to the first set of "star 1" windings and dq2 to the second set of "star 2" windings . Due to this advantage, the double-dq model is the model adopted in this work[MES22].

I.7 Works carried out for the control of the six-phase asynchronous machine

There are several control techniques have been studied to control the asynchronous machine. They have been developed to replace vector control, such as direct torque control DTC and

Sliding Mode Control and Sliding Mode Control SMC, providing good robustness against parameters variations. Among the techniques applied to the control of the asynchronous machine, the following:

- ✓ **Vector Controlin [DJA13] presented by DjaborebbiAmina;** "This work focuses on the study and control of a double-star asynchronous machine. Special attention is given to the implementation of speed control for this type of machine."
- ✓ **Field-Oriented Control in [ALI17] presented by Ali Ahmed;***This work focuses on implementing field-oriented control strategies for a dual-star induction motor. The study aims to achieve decoupled control of torque and flux, improving system efficiency.*
- ✓ **Vector Control in [MES22] presented by HamzaMesai Ahmed.**The main objective of this work is to present solutions to improve the performance and increase the control reliability of the machine.
- ✓ **Direct Torque Control in [KIY20] presented by LaggounLouanasse;** *This work focuses on the study and enhancement of direct torque control (DTC) applied to a permanent magnet double-star synchronous machine (6PHI-MAP) supplied by two voltage inverters. The objective is to improve control performance and dynamic behavior.*
- ✓ **Direct Torque Control in [BEN15] presented by Benamara Rania;** *This study investigates direct torque control techniques applied to induction machines. The main focus is on improving the dynamic response and minimizing torque ripple.*
- ✓ **Sliding Mode Control in [KHI16] presented by KhireddineYacine;** *The research explores the application of sliding mode control to asynchronous motors. Emphasis is placed on enhancing robustness against parameter variations and external disturbances.*
- ✓ **Sliding Mode Control in [AMI12] presented by AmimeurHocine;** *This research contributes to the control of a double-star asynchronous machine using sliding mode control techniques. The study emphasizes the robustness of the control strategy against system uncertainties and external disturbances.*
- ✓ **Sensorless Control Methods in [HAM18] presented by HamdiSoumaya;** *This thesis presents a comparative study of sensorless control algorithms for asynchronous machines. Special attention is given to the accuracy of speed estimation under variable load conditions.*

- ✓ **Fuzzy Logic Control in [BOU19] presented by Bouzid Lynda;** *The research introduces fuzzy logic-based control techniques for double-star induction machines. The objective is to enhance adaptability and performance under nonlinear operating conditions.*

I.8 Sliding mode control in the literature

These research studies explore the applications of Sliding Mode Control (SMC) in various fields. In [Zahr17] A. K. Abdul Zahra from the University of Basrah designed a robust control system for suspension systems, reducing vibrations and improving performance . In[Maj20] H. S. Majid** from the University of Technology, Iraq, developed a sliding mode control strategy for an artificial finger, achieving a 90% agreement between simulations and experimental tests. In Algeria, [Maa19] F. Maallem from the University of Mohamed Boudiaf analyzed the impact of landslides on the urban fabric of Boualssouf neighborhood in Constantine, while M. Maallem** studied the structural risks of landslides and proposed mitigation strategies. [Shi18] H. Shiltagh from the University of Kufa enhanced voltage regulator control using Sliding Mode Control, leading to better voltage stability in electrical systems..V. Utkin [Utk93]from Moscow State University introduced the fundamental theory of Sliding Mode Control, which became a key reference in nonlinear control. S. Drakunov [Utk93]from Tulane University proposed SMC techniques for discrete-time systems, improving their robustness and stability. At the University of Alabama, Y. Shtessel [Sht12] developed super-twisting SMC controllers to reduce chattering and enhance system performance. Finally, C. Edwards [Edw00]from the University of Exeter designed fault-tolerant SMC systems for aerospace applications, ensuring stability even under actuator failures. These contributions highlight the significance of Sliding Mode Control in diverse engineering applications.

I.9 Conclusion

This chapter presents a state-of-the-art review of the history, structure, and operating principles of electric machines, with a focus on existing topologies, different modeling approaches, and the most widely used control strategies for multiphase systems. The advantages and disadvantages of each strategy are discussed based on previous research conducted on the most common control techniques in these systems.

The next chapter will cover the modeling and vector control of a six-phase asynchronous machine powered by two voltage inverters.

CHAPTER 2

Study and modeling of the six-phase Induction machine

2.1 introduction

The modeling of any system is essential for the application of a specific control. In this chapter, we will focus on modeling the different parts of the studied system, which consists of the six-phase induction machine (6PH-IM), the converters, and the DC bus. In fact, modeling an electrical machine requires highly complex equations, as the winding distribution and the specific geometry of the six-phase induction machine make its model difficult to implement. However, adopting certain simplifying assumptions allows us to overcome this difficulty.

In this chapter, the modeling of the six-phase induction machine fed by two power converters will be presented. In this study, an angular offset of **α = 30°** (the angle between adjacent phases) is considered. The developed model aims to accurately represent the dynamic behavior of the machine while ensuring a balance between precision and computational efficiency. Finally, simulation results will be presented and analyzed in detail to validate the proposed modeling approach and assess its performance under different operating conditions.

2.2 Six phase machine desTliption:

The six-phase induction motor (6PH-IM) consists of a stator equipped with two identical three-phase windings, which are offset by an electrical angle of α = 30°. The rotor is of the squirrel-cage type.Figure 2.1 provides a schematic representation of the windings in the 6PH-IM. The angles θr and (θr − α) indicate the rotor's position relative to the first star winding (phase as1) and the second star winding (phase as2), respectively. Quantities associated with the two star windings (1 and 2) will be denoted using the indices 1 and 2, respectively.

The three-phase asynchronous motor with a double stator is an electric machine featuring two fixed stator windings and a movable rotor winding. These two stators are positioned at an angular offset from each other, with each containing three identical windings. Their axes are separated by an equal electrical angle $2\pi \div 3$ in space and are embedded in the slots of the magnetic circuit. Each stator winding is powered by a balanced three-phase current system, generating a rotating magnetic field that moves through the air gap.The speed of this rotating field depends on the

number of pole pairs in the machine and the frequency of the stator currents, expressed as: [*KER*13]

$$\Omega = \omega s / P \quad 01$$

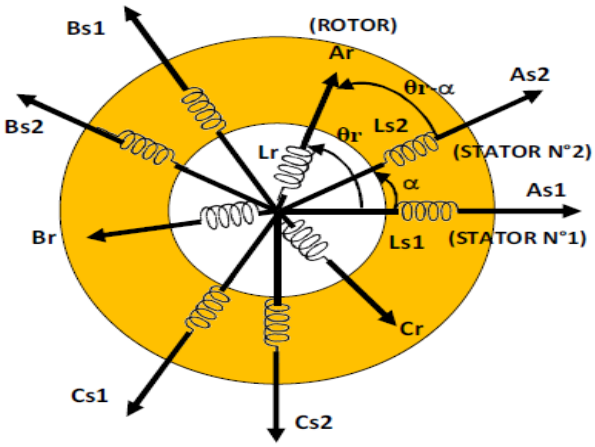

Figure 2.1 : Schematic representation of the 6PH-IM windings

2.3 Simplifying assumptions:

Before modeling the machine, certain simplifying assumptions are made to address the complexities associated with its behavior. The adopted model is based on the following assumptions

- The air gap is uniform, and the effect of slotting (Encochage) is neglected.
- The electromotive forces (EMF) generated by each phase of the two windings have a sinusoidal spatial distribution.
- The machine exhibits perfect symmetry in both its magnetic and electrical properties.
- Magnetic saturation, hysteresis losses, and eddy currents are disregarded.
- The resistance of the windings remains constant, independent of temperature variations, and the skin effect is neglected
- The mutual inductance between the two stator windings (star 1 and star 2) is assumed to be negligible.
- The machine operates under balanced conditions. [*KER 13*]

2.4 Modeling of the six-phase machine

2.4.1 Electrical equation of the six-phase machine:

The voltage equations of the six-phase machine desTlibe, for each winding, the total voltage drop, which includes both the ohmic drop and the inductive drop caused by the magnetic flux.[Bos 09]

For the star configuration:1:

$$\begin{cases} U_{as1} = R_{s1} i_{as1} + \dfrac{d\varphi_{as1}}{dt} \\ U_{bs1} = R_{s1} i_{bs1} + \dfrac{d\varphi_{bs1}}{dt} \\ U_{cs1} = R_{s1} i_{cs1} + \dfrac{d\varphi_{cs1}}{dt} \end{cases} \quad (2.1)$$

For star 2:

$$\begin{cases} U_{as2} = R_{s2} i_{as2} + \dfrac{d\varphi_{as2}}{dt} \\ U_{bs2} = R_{s2} i_{bs2} + \dfrac{d\varphi_{bs2}}{dt} \\ U_{cs2} = R_{s2} i_{cs2} + \dfrac{d\varphi_{cs2}}{dt} \end{cases} \quad (2.2)$$

For rotor:

$$\begin{cases} 0 = U_{ar} = R_r i_{ar} + \dfrac{d\varphi_{ar}}{dt} \\ 0 = U_{br} = R_r i_{br} + \dfrac{d\varphi_{br}}{dt} \\ 0 = U_{cr} = R_r i_{cr} + \dfrac{d\varphi_{cr}}{dt} \end{cases} \quad (2.3)$$

In matrix form, we have:

For star 1: $[U_{s1}]=[R_{s1}][i_{s1}]+\frac{d}{dt}[\varphi_{s1}]$ (2.4)

For star 2: $[U_{s2}]=[R_{s2}][i_{s2}]+\frac{d}{dt}[\varphi_{s2}]$ (2.5)

For rotor: $[U_r]=[R_r][i_r]+\frac{d}{dt}[\varphi_r]$ (2.6)

With :

$$[U_{s1}]=\begin{bmatrix}U_{as1}\\U_{bs1}\\U_{cs1}\end{bmatrix};[U_{s2}]=\begin{bmatrix}U_{as2}\\U_{bs2}\\U_{cs2}\end{bmatrix};[U_r]=\begin{bmatrix}U_{ar}\\U_{br}\\U_{cr}\end{bmatrix} \quad (2.7)$$

$[U_{s1}]$: Star 1 voltage matrix ;

$[U_{s2}]$: Star 2 voltage matrix;

$[U_r]$: Rotor Voltage Matrix.

With :

$$[i_{s1}]=\begin{bmatrix}i_{as1}\\i_{bs1}\\i_{cs1}\end{bmatrix};[i_{s2}]=\begin{bmatrix}i_{as2}\\i_{bs2}\\i_{cs2}\end{bmatrix};[i_r]=\begin{bmatrix}i_{ar}\\i_{br}\\i_{cr}\end{bmatrix} \quad (2.8)$$

$[i_{s1}]$:Current matrix of star 1;

$[i_{s2}]$: Current matrix of star 2;

$[i_r]$: Rotor current matrix.

With :

$$R_{as1}=R_{bs1}=R_{cs1}\ ;\ R_{as2}=R_{bs2}=R_{cs2}\ \text{et}\ R_{ar}=R_{br}=R_{cr} \quad (2.9)$$

$$[R_{s1}]=\begin{bmatrix}R_{as1}&0&0\\0&R_{bs1}&0\\0&0&R_{cs1}\end{bmatrix};\ [R_{s2}]=\begin{bmatrix}R_{as2}&0&0\\0&R_{bs2}&0\\0&0&R_{cs2}\end{bmatrix};[R_r]=\begin{bmatrix}R_{ar}&0&0\\0&R_{br}&0\\0&0&R_{cr}\end{bmatrix} \quad (2.10)$$

$[R_{s1}]$:Resistance of a star phase 1;

$[R_{s2}]$: Resistance of a phase of star 2;

$[R_r]$: Resistance of a phase of the rotor.

$$[\varphi_{s1}]=\begin{bmatrix}\varphi_{as1}\\ \varphi_{bs1}\\ \varphi_{cs1}\end{bmatrix};[\varphi_{s2}]=\begin{bmatrix}\varphi_{as2}\\ \varphi_{bs2}\\ \varphi_{cs2}\end{bmatrix};[\varphi_r]=\begin{bmatrix}\varphi_{ar}\\ \varphi_{br}\\ \varphi_{cr}\end{bmatrix} \quad (2.11)$$

$[\varphi_{s1}]$: Flux matrix of star 1;

$[\varphi_{s2}]$: Flux matrix of star 2;

$[\varphi_r]$: Rotor flux matrix.

II.4.2 Magnetic equations of the six-phase machine:

The stator and rotor fluxes are determined based on the currents, self-inductances, and mutual inductances, using the matrix derived from the following equations:

$$[L(\theta)]=\begin{bmatrix}[L_{s1,s1}][M_{s1,s2}][M_{s1,r}]\\ [M_{s2,s1}][L_{s2,s2}][M_{s2,r}]\\ [M_{r,s1}][M_{r,s2}][L_{r,r}]\end{bmatrix} \quad (2.12)$$

$$\begin{bmatrix}[\varphi_{s1}]\\ [\varphi_{s2}]\\ [\varphi_r]\end{bmatrix}=[L(\theta)]\begin{bmatrix}[i_{s1}]\\ [i_{s2}]\\ [i_r]\end{bmatrix} \quad (2.13)$$

The sub-matrices of the inductance matrix are expressed as follows:

$$[L_{s1,s1}]=\begin{bmatrix}(L_{s1}+L_{ms}) & L_{ms}\cos\left(\frac{2\pi}{3}\right) & L_{ms}\cos\left(\frac{4\pi}{3}\right)\\ L_{ms}\cos\left(\frac{4\pi}{3}\right) & (L_{s1}+L_{ms}) & L_{ms}\cos\left(\frac{2\pi}{3}\right)\\ L_{ms}\cos\left(\frac{2\pi}{3}\right) & L_{ms}\cos\left(\frac{4\pi}{3}\right) & (L_{s1}+L_{ms})\end{bmatrix} \quad (2.14)$$

$$[L_{s2,s2}]=\begin{bmatrix}(L_{s2}+L_{ms}) & L_{ms}\cos\left(\frac{2\pi}{3}\right) & L_{ms}\cos\left(\frac{4\pi}{3}\right)\\ L_{ms}\cos\left(\frac{4\pi}{3}\right) & (L_{s2}+L_{ms}) & L_{ms}\cos\left(\frac{2\pi}{3}\right)\\ L_{ms}\cos\left(\frac{2\pi}{3}\right) & L_{ms}\cos\left(\frac{4\pi}{3}\right) & (L_{s2}+L_{ms})\end{bmatrix} \quad (21.5)$$

$$[L_{r,r}]=\begin{bmatrix} (L_r+L_{mr}) & L_{mr}\cos\left(\frac{2\pi}{3}\right) & L_{mr}\cos\left(\frac{4\pi}{3}\right) \\ L_{mr}\cos\left(\frac{4\pi}{3}\right) & (L_r+L_{mr}) & L_{mr}\cos\left(\frac{2\pi}{3}\right) \\ L_{mr}\cos\left(\frac{2\pi}{3}\right) & L_{mr}\cos\left(\frac{4\pi}{3}\right) & (L_r+L_{mr}) \end{bmatrix}$$

(2.16)

$$[M_{s1,s2}]=\begin{bmatrix} L_{ms}\cos(\alpha) & L_{ms}\cos\left(\alpha+\frac{2\pi}{3}\right) & L_{ms}\cos\left(\alpha+\frac{4\pi}{3}\right) \\ L_{ms}\cos\left(\alpha+\frac{4\pi}{3}\right) & L_{ms}\cos(\alpha) & L_{ms}\cos\left(\alpha+\frac{2\pi}{3}\right) \\ L_{ms}\cos\left(\alpha+\frac{2\pi}{3}\right) & L_{ms}\cos\left(\alpha+\frac{4\pi}{3}\right) & L_{ms}\cos(\alpha) \end{bmatrix} \quad (2.17)$$

$$[M_{s1,r}]=\begin{bmatrix} L_{sr}\cos(\theta_r) & L_{sr}\cos\left(\theta_r+\frac{2\pi}{3}\right) & L_{sr}\cos\left(\theta_r+\frac{4\pi}{3}\right) \\ L_{sr}\cos\left(\theta_r+\frac{4\pi}{3}\right) & L_{sr}\cos(\theta_r) & L_{sr}\cos\left(\theta_r+\frac{2\pi}{3}\right) \\ L_{sr}\cos\left(\theta_r+\frac{2\pi}{3}\right) & L_{sr}\cos\left(\theta_r+\frac{4\pi}{3}\right) & L_{sr}\cos(\theta_r) \end{bmatrix} \quad (2.18)$$

$$[M_{s2,r}]=\begin{bmatrix} L_{sr}\cos(\theta_r-\alpha) & L_{sr}\cos\left(\theta_r-\alpha+\frac{2\pi}{3}\right) & L_{sr}\cos\left(\theta_r-\alpha+\frac{4\pi}{3}\right) \\ L_{sr}\cos\left(\theta_r-\alpha+\frac{4\pi}{3}\right) & L_{sr}\cos(\theta_r-\alpha) & L_{sr}\cos\left(\theta_r-\alpha+\frac{2\pi}{3}\right) \\ L_{sr}\cos\left(\theta_r-\alpha+\frac{2\pi}{3}\right) & L_{sr}\cos\left(\theta_r-\alpha+\frac{4\pi}{3}\right) & L_{sr}\cos(\theta_r-\alpha) \end{bmatrix} \quad (2.19)$$

$$[M_{s2,s1}]=[M_{s1,s2}]^t \;;\; [M_{r,s1}]=[M_{s1,r}]^t \;;\; [M_{r,s2}]=[M_{s2,r}]^t \quad (2.20)$$

$$L_{ms}=L_{mr}=L_{sr}=\frac{2}{3}L_m \quad (2.21)$$

With :

L_{s1} :The self-inductance of the stator1;

L_{s2} : The self-inductance of the stator2;

L_r : The self-inductance of a phase of the rotor;

L_{ms} : The maximum value of the stator mutual inductance coefficients;

L_{mr} : The maximum value of the rotor mutual inductance coefficients;

L_{sr} : The maximum value of the mutual inductance coefficients between a star and the rotor.

II.4.3 Magnetic energy of the six-phase machine:

We can calculate the magnetic energy stored in the rotor from the following expression.

$$w_{mag} = \frac{1}{2}\left([i_{s1}]^t[\varphi_{s1}] + [i_{s2}]^t[\varphi_{s2}] + [i_r]^t[\varphi_r]\right) \quad (2.22)$$

II.4.4 Expression of the electromagnetic torque of the six-phase machine:

The expression of the electromagnetic torque is obtained by the derivation of the co energy with respect to the magnetic angle .

$$C_{em} = \frac{d}{d\theta_{mag}} w_{mag} = p\frac{d}{d\theta_e} w_{mag} \quad (2.23)$$

With :

p : pole pair number.

θ_{mag} : magnetic angle.

θ_e : electric angle

$$C_{em} = \frac{p}{2}\left([i_{s1}]\frac{d}{d\theta_r}[L_{s1,r}][i_r]^t + [i_{s2}]\frac{d}{d\theta_r}[L_{s2,r}][i_r]^t\right) \quad (2.24)$$

With :

θ_r : Rotor position relative to star 1 [rd].

2.4.5 Mechanical equation of the six-phase machine:

$$J\frac{d\Omega}{dt} = C_{méc} = C_g - C_{em} - C_f \quad (2.25)$$

With :

$$\Omega = \frac{\omega_r}{p} \quad (2.26)$$

On the other hand :

$$\omega_r = \frac{d\theta_r}{dt} \quad (2.27)$$

2.5 Park-based transformation:

The Park model is based on transforming a three-phase system with axes (a, b, c) into an equivalent two-phase system with axes (d, q) while preserving the same magnetomotive force (MMF).

A second transformation, known as the modified Park transformation, allows power to be preserved when converting from a three-phase system to a two-phase system or vice versa

The homopolar component does not contribute to this transformation, so the homopolar axis can be chosen orthogonal to the (od, oq) plane (LOU 14)..

2.5.1 Park's matrix in general:

For star 1 is defined as follows:

$$\left[P(\theta_{s1})\right]=\sqrt{\frac{2}{3}}\begin{bmatrix}\cos(\theta) & \cos\left(\theta-\frac{2}{3}\right) & \cos\left(\theta+\frac{2}{3}\right)\\ -\sin(\theta) & -\sin\left(\theta-\frac{2}{3}\right) & -\sin\left(\theta+\frac{2}{3}\right)\\ \frac{1}{\sqrt{2}} & \frac{1}{\sqrt{2}} & \frac{1}{\sqrt{2}}\end{bmatrix} \quad (2.28)$$

$$\left[P(\theta_{s1})\right]^{-1}=\sqrt{\frac{2}{3}}\begin{bmatrix}\cos(\theta) & -\sin(\theta) & \frac{1}{\sqrt{2}}\\ \cos\left(\theta-\frac{2}{3}\right) & -\sin\left(\theta-\frac{2}{3}\right) & \frac{1}{\sqrt{2}}\\ \cos\left(\theta+\frac{2}{3}\right) & -\sin\left(\theta+\frac{2}{3}\right) & \frac{1}{\sqrt{2}}\end{bmatrix} \quad (2.29)$$

• For star 2 and the rotor, we replace in (II.28) et (II.29) θ by $(\theta-\alpha)$ and then by $(\theta_{gl}=\theta-\theta_r)$ respectively.

2.6 Choice of benchmark:

Three types of frames of reference are interesting in practice, the choice of the frame of reference made according to the problem to be studied [ABA22]

.26.1 Frame of reference linked to the stator ($\omega coor$=0).

$$\frac{d\theta_s}{dt} = 0 \tag{2.30}$$

$$\theta_s = \theta_r + \theta \tag{2.31}$$

$$\frac{d\theta_s}{dt} = 0 = \frac{d\theta_r}{dt} + \frac{d\theta}{dt} \tag{2.32}$$

$$\frac{d\theta_r}{dt} = -\frac{d\theta}{dt} = -p\Omega \tag{2.33}$$

This reference frame is stationary with respect to the stator, used for the study of starting and braking of alternating current machines with connection of resistors

2.6.2 Referential related to the rotor ($\omega_{coor} = \omega_r$).

$$\frac{d\theta_r}{dt} = 0 \tag{2.34}$$

$$\frac{d\theta_s}{dt} = \frac{d\theta}{dt} = p\Omega \tag{2.35}$$

This reference frame is stationary with respect to the rotor, used for the study of transient regimes in asynchronous and synchronous machines.

2.6.3 Referential to the rotating field

$$\frac{d\theta}{dt} = \omega_s \tag{2.36}$$

$$\frac{d\theta}{dt} = \omega_s - p\Omega \tag{2.37}$$

The latter is used to realize the vector control due to the fact that the manipulated quantities become continuous.

2.7 Park model of the 6PH-IM:

In this study, we selected this reference frame for modeling the six-phase induction machine (6PH-IM) due to its widespread use in speed, torque, and other control applications. This reference frame provides a continuous representation of the machine's quantities, making control implementation more effective.

The d-q coordinate system remains fixed relative to the electromagnetic field generated by the stator windings [MES19**]** The Park transformation is derived by projecting the machine's three-phase quantities onto two perpendicular axes, d and q.

$$X_{dqo} = P(\theta_s) X_{abc} \tag{2.38}$$

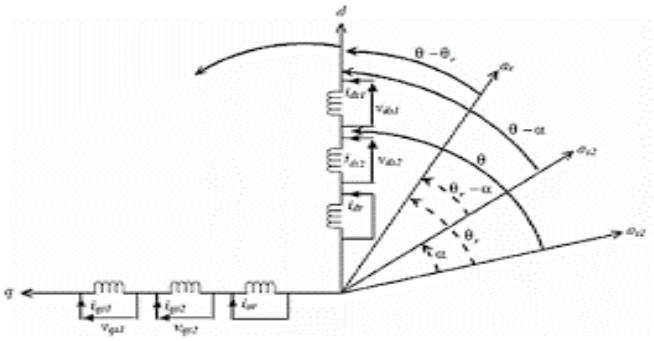

Figure 2.2: The generalized model of 6PH-IM along the axes

2.7.1 Matrix equation of 6PH-IM with Park transformation

$$\begin{cases} U_{ds1} = R_{s1} i_{ds1} + \dfrac{d}{dt}\varphi_{ds1} - \omega_s \varphi_{qs1} \\ U_{qs1} = R_{s1} i_{qs1} + \dfrac{d}{dt}\varphi_{qs1} + \omega_s \varphi_{ds1} \\ U_{ds2} = R_{s2} i_{ds2} + \dfrac{d}{dt}\varphi_{ds2} - \omega_s \varphi_{qs2} \\ U_{qs2} = R_{s2} i_{qs2} + \dfrac{d}{dt}\varphi_{qs2} + \omega_s \varphi_{ds2} \\ U_{dr} = R_r i_{dr} + \dfrac{d}{dt}\varphi_{dr} - \omega_{gl} \varphi_{qr} \\ U_{qr} = R_r i_{qr} + \dfrac{d}{dt}\varphi_{qr} + \omega_{gl} \varphi_{dr} \end{cases} \tag{2.39}$$

Or :

$$\omega_{gl} = \omega_s - \omega_r \tag{2.40}$$

The components of the stator and rotor fluxes are expressed as follows:

$$\begin{cases} \phi_{ds1} = L_{s1} i_{ds1} + L_m \left(i_{ds1} + i_{ds2} + i_{dr} \right) \\ \phi_{qs1} = L_{s1} i_{qs1} + L_m \left(i_{qs1} + i_{qs2} + i_{qr} \right) \\ \phi_{ds2} = L_{s2} i_{ds2} + L_m \left(i_{ds1} + i_{ds2} + i_{dr} \right) \\ \phi_{qs2} = L_{s2} i_{qs2} + L_m \left(i_{qs1} + i_{qs2} + i_{qr} \right) \\ \phi_{dr} = L_r i_{dr} + L_m \left(i_{ds1} + i_{ds2} + i_{dr} \right) \\ \phi_{qr} = L_r i_{qr} + L_m \left(i_{qs1} + i_{qs2} + i_{qr} \right) \end{cases} \quad (2..41)$$

With :

$$\omega_s = \frac{d\theta}{dt} \quad (2.42)$$

$$\omega_r = \frac{d\theta_r}{dt} \quad (2.43)$$

$$p\Omega = \frac{d\theta}{dt} - \frac{d\theta_r}{dt} = \omega_s - \omega_r \quad (2.44)$$

With :

$L_{s1} + L_m$: Cyclic self-inductance of stator 1.

$L_{s2} + L_m$: Cyclic self-inductance of stator 2.

$L_r + L_m$: Rotor cyclic self-inductance.

$L_m = \frac{3}{2} L_{ms} = \frac{3}{2} L_{mr} = \frac{3}{2} L_{sr}$: Cyclic mutual inductance between star 1 and 2 and the rotor.

2.8 Modeling in the form of an equation of state

Putting the system in the form of a state, we find:

$$\left[\dot{I} \right] = [L]^{-1} \left([B][U] - \omega_{gl} [C][I] - [D][I] \right) \quad (2.45)$$

Or :

$$[B] = diag[1 \quad 1 \quad 1 \quad 1 \quad 0 \quad 0] \quad (2.46)$$

Command vector:

$$[U] = \left[U_{ds1}, U_{qs1}, U_{ds2}, U_{qs2}, U_{dr}, U_{qr} \right]^t \quad (2.47)$$

State vector :

$$[I] = \left[i_{ds1}, i_{qs1}, i_{ds2}, i_{qs2}, i_{dr}, i_{qr} \right]^t \quad (2.48)$$

$$\left[\dot{I}\right]=\frac{d}{dt}[I] \tag{2.49}$$

$$[L]=\begin{bmatrix} (L_{s1}+L_m) & 0 & L_m & 0 & L_m & 0 \\ 0 & (L_{s2}+L_m) & 0 & L_m & 0 & L_m \\ L_m & 0 & (L_{s2}+L_m) & 0 & L_m & 0 \\ 0 & L_m & 0 & (L_{s2}+L_m) & 0 & L_m \\ L_m & 0 & L_m & 0 & (L_r+L_m) & 0 \\ 0 & L_m & 0 & L_m & 0 & (L_r+L_m) \end{bmatrix} \tag{2.50}$$

$$[C]=\begin{bmatrix} 0 & 0 & 0 & 0 & 0 & 0 \\ 0 & 0 & 0 & 0 & 0 & 0 \\ 0 & 0 & 0 & 0 & 0 & 0 \\ 0 & 0 & 0 & 0 & 0 & 0 \\ 0 & -L_m & 0 & -L_m & 0 & -(L_r+L_m) \\ L_m & 0 & L_m & 0 & (L_r+L_m) & 0 \end{bmatrix} \tag{2.51}$$

$$[D]=\begin{bmatrix} R_{s1} & -\omega_s(L_{s1}+L_m) & 0 & -\omega_s L_m & 0 & -\omega_s L_m \\ \omega_s(L_{s1}+L_m) & R_{s1} & \omega_s L_m & 0 & \omega_s L_m & 0 \\ 0 & -\omega_s L_m & R_{s2} & -\omega_s(L_{s2}+L_m) & 0 & -\omega_s L_m \\ \omega_s L_m & 0 & -\omega_s(L_{s2}+L_m) & R_{s2} & \omega_s L_m & 0 \\ 0 & 0 & 0 & 0 & R_r & 0 \\ 0 & 0 & 0 & 0 & 0 & R_r \end{bmatrix} \tag{2.52}$$

2.9 Expressions of the absorbed power and electromagnetic torque

The power of the 6PH-IM in the system of axes (d, q), while neglecting the homopolar components is expressed by:

$$P_a = V_{ds1}i_{ds1} + V_{qs1}i_{qs1} + V_{ds2}i_{ds2} + V_{qs2}i_{qs2} \tag{2.53}$$

By replacing the voltages $(V_{ds1}, V_{qs1}, V_{ds2}, V_{ds2})$ by their expressions in the equation we find:

$$P_a = \underbrace{\left[R_{s1}i_{ds1}^2 + R_{s1}i_{qs1}^2 + R_{s2}i_{ds2}^2 + R_{s2}i_{qs2}^2\right]}_{Terme\ 1} + \underbrace{\left(\frac{d\varphi_{ds1}}{dt}i_{ds1} + \frac{d\varphi_{qs1}}{dt}i_{qs1} + \frac{d\varphi_{ds2}}{dt}i_{ds2} + \frac{d\varphi_{qs2}}{dt}i_{qs2}\right)}_{Terme\ 2} + \underbrace{\omega_s\left(\varphi_{ds1}i_{qs1} - \varphi_{qs1}i_{ds1} + \varphi_{ds2}i_{qs2} - \varphi_{qs2}i_{ds2}\right)}_{Terme\ 3} \tag{2.54}$$

This expression is made up of three terms, the first term corresponds to the losses by Joule effect, the second term represents the variation of the electromagnetic energy (energy reserve), the last term is the stored electromagnetic power (Pem).

By the comparison between the universal relation of electromagnetic power and the third term of supplied power:

$$P_{em} = \omega_s \left(\varphi_{ds1} i_{qs1} - \varphi_{qs1} i_{ds1} + \varphi_{ds2} i_{qs2} - \varphi_{qs2} i_{ds2} \right) \tag{2.55}$$

We find:

$$C_{em} = p\left(\varphi_{ds1} i_{qs1} - \varphi_{qs1} i_{ds1} + \varphi_{ds2} i_{qs2} - \varphi_{qs2} i_{ds2} \right) \tag{2.56}$$

$$C_{em} = \frac{P_{em}}{\Omega_s} = p \frac{P_{em}}{\omega_s} \tag{2.57}$$

The electromagnetic torque expressions can be written as follows. By replacing the expressions (II.40) in (II.56), we get :

$$C_{em} = pL_m \left\{ \left(i_{qs1} + i_{qs2} \right) i_{dr} - \left(i_{ds1} + i_{ds2} \right) i_{qr} \right\} \tag{2.58}$$

From the rotor flux equations (φ_{dr} et φ_{qr}) expressed by (III.40), we get

$$i_{dr} = \frac{1}{L_m + L_r} \left[\varphi_{dr} - L_m \left(i_{ds1} + i_{ds2} \right) \right] \tag{2.59}$$

$$i_{qr} = \frac{1}{L_m + L_r} \left[\varphi_{qr} - L_m \left(i_{qs1} + i_{qs2} \right) \right] \tag{2.60}$$

By replacing (III.59) and (III.60) in the equation (III.58), we will have the relation of the electromagnetic torque in the Park frame (d, q) as follows:

$$C_{em} = p \frac{L_m}{L_m + L_r} \left\{ \left(i_{qs1} + i_{qs2} \right) \varphi_{dr} - \left(i_{ds1} + i_{ds2} \right) \varphi_{qr} \right\} \tag{2.61}$$

2.10 Simulation of the 6PH-IM powered by sinusoidal voltages

The simulation consists of implementing the electromechanical model of 6PH-IM under the Mat lab/Simulink environment[31].

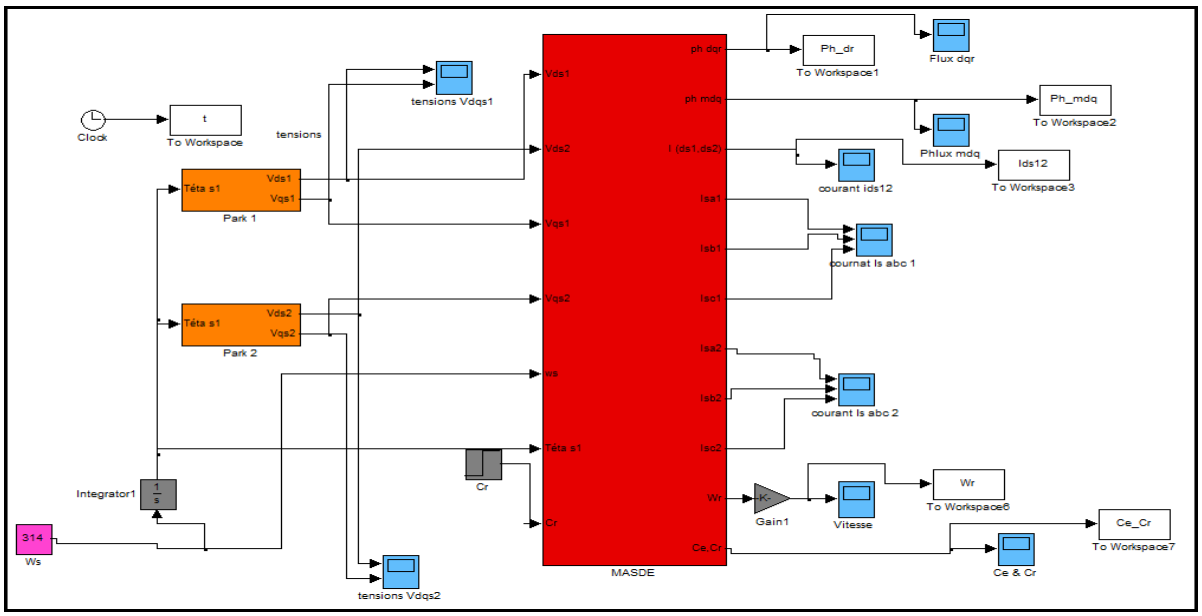

The simulation block diagram**2.3: Figure**

2.10.1 Simulation Results:

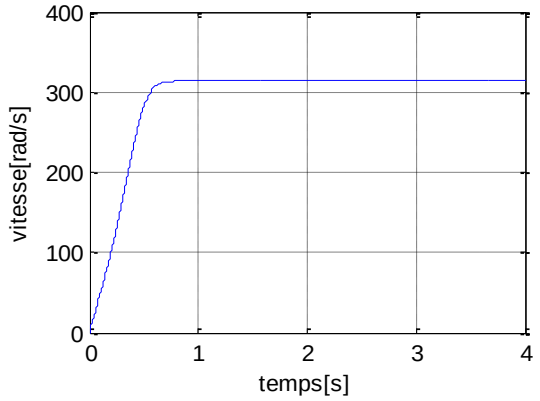

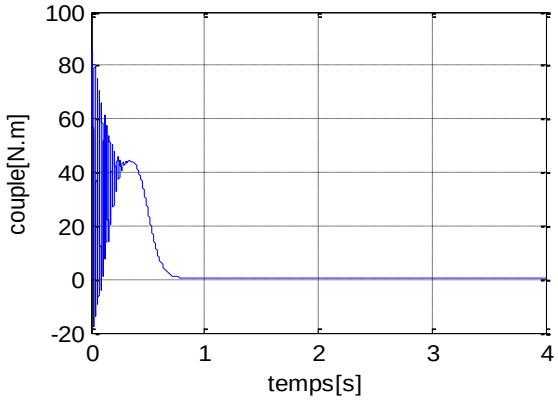

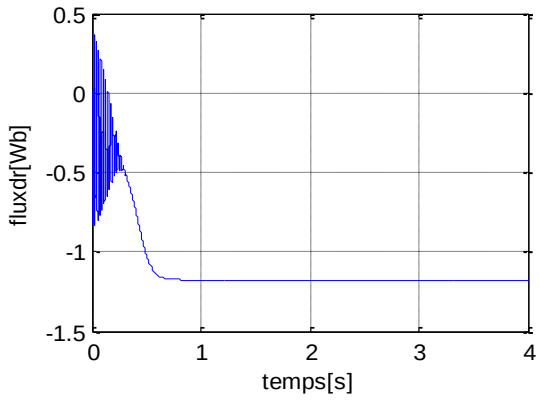

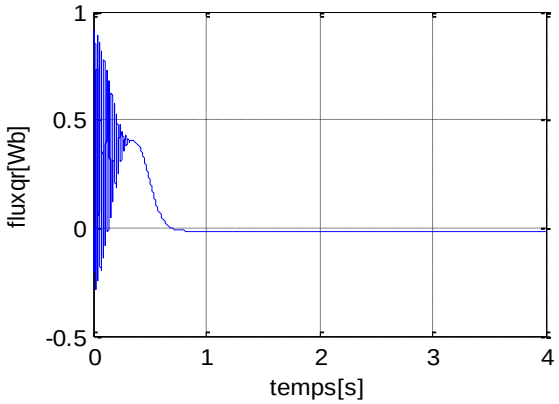

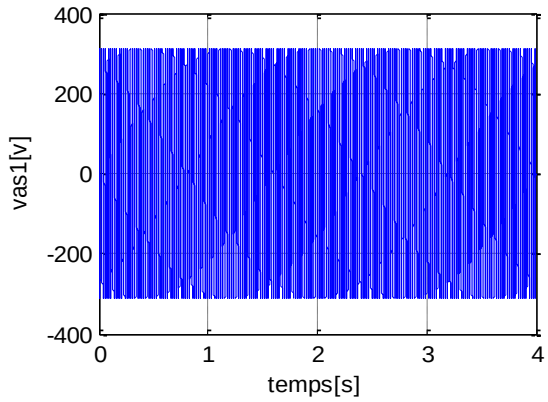

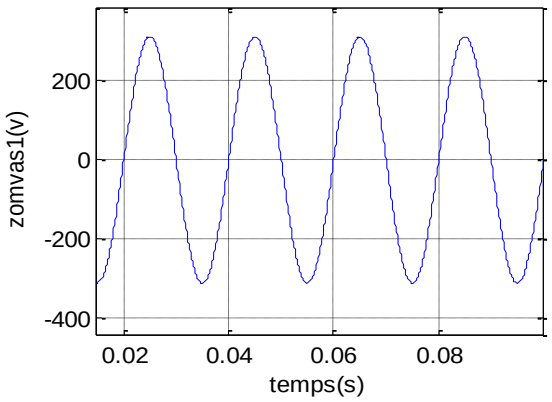

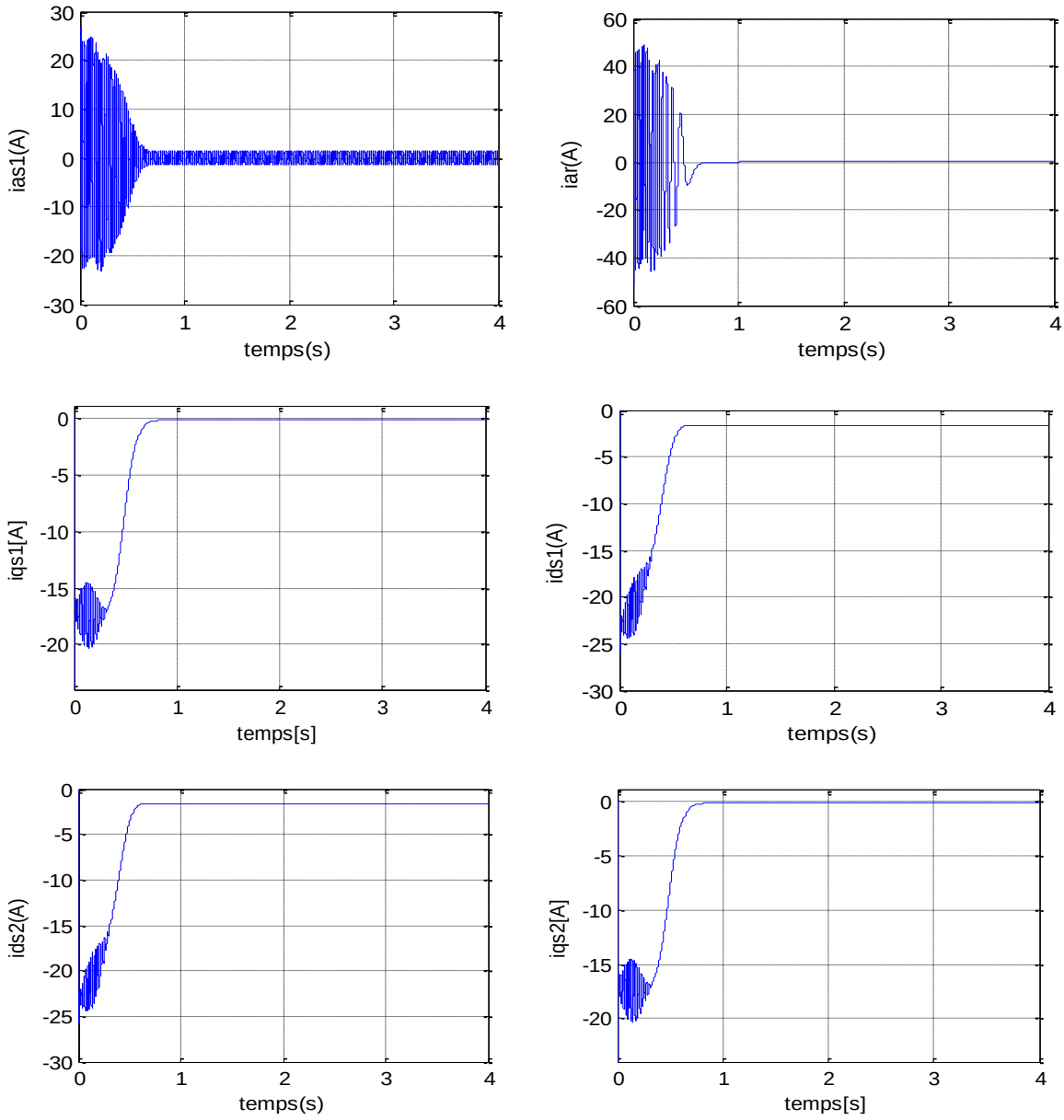

Figure 2.4: Performances of the six phase induction machine in starting state without load

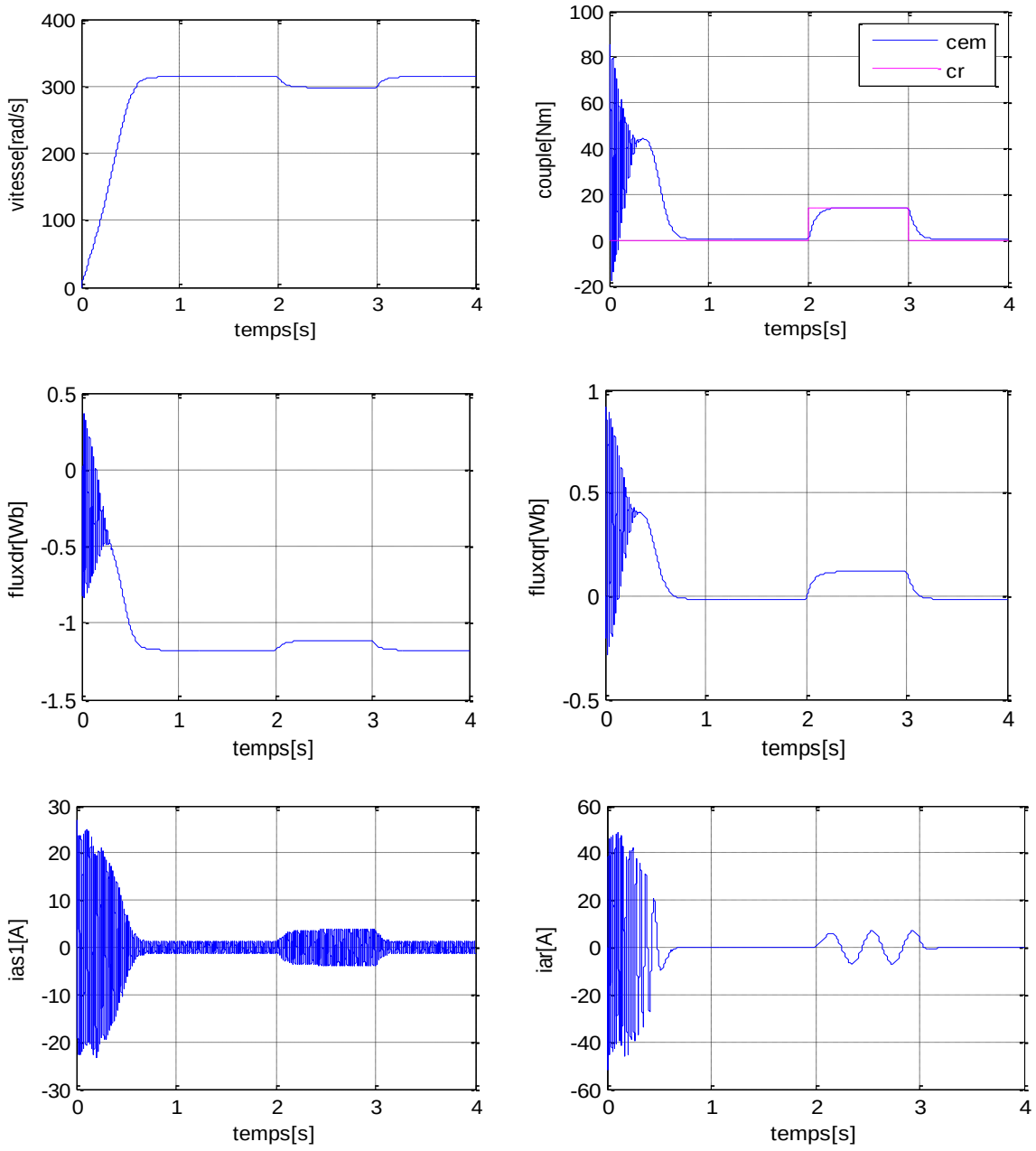

Figure II.5: Performances of the six phase induction machine with load of Cr=14 N.m between 2s et 3s

2.10.2 Discussion of the results

We simulated the operation of the asynchronous double stator machine powered directly from the standard network (220/ 380V, 50Hz), empty and loaded.

The simulation results given by the figures (Figure II.5 and Figure II.4), these figures represent the evolution of some fundamental variables of the asynchronous machine, namely the speed of rotation (ω_r), the electromagnetic torque (Cem), stator phase currents (i_{sa1}, i_{sa2}), currents according to axes d and q (i_{sd1} i_{sd2}, i_{sq1} i_{sq2}) and rotor flux (flux rd, flux rq).

At start-up and during the transient speed, the speed increases and evolves in an almost linear manner and reaches 313.8 rad/s à $t \approx 0.8$s (marking the beginning of steady-state operation).

The electromagnetic torque, at the beginning reaches its maximum value of 85.4N.m, and presents oscillations that disappear after 0.4 s, where it reaches 42.4 N.m, then it decreases in an almost linear way and stabilizes at its minimum value of 0.314 N.m, which is due to friction. The stator currents (stars 1 and 2) show excessive exceedances inducing strong current calls of about 4 times the nominal current, but which disappears after some alternations to give rise to sine forms of constant amplitude. The stator currents along the direct and quadrature axes evolve in a manner roughly analogous to the evolution of the velocity; nevertheless, there are slight oscillations at the level of the latter during approximately 0.3s. The evolution of rotor flows is almost identical to that of the electromagnetic couple.

When a load torque of Cr = 14 N·m is applied between t = 2s and 3s (under motor operating conditions), the speed and d-q axis currents decrease and stabilize at wr = 298 rad/s, $i_{ds1} = i_{ds2} = -1.97$ A, and $i_{qs1} = i_{qs2} = -4.13$ A, respectively.

Conversely, increases are observed in electromagnetic torque, stator currents (stars 1 and 2), and rotor fluxes in the d-q reference frame, settling at Cem = 14.33 N·m (slightly above the applied torque), $i_{as1} = i_{as2} = 3.74$ A, flux dr = −1.11 Wb, and flux qr = 0.11 Wb.

In motor operation, the machine slip is slightly higher compared to the no-load case. The supply voltage V_{as1} and stator current $i_{as1}$are almost in phase and of the same sign; however, the offset behind the current in relation to the voltage due to the inductive effect of the machine, the two quantities are of the same sign means that the direction of transition of the power is positive.

.211 Conclusion:

In this chapter, we focused on the modeling of the six-phase induction machine (6PH-IM) operating as a motor. This modeling enabled us to establish a mathematical representation of the machine, where the complexity was significantly reduced by adopting several simplifying assumptions. To facilitate the implementation of the system equations in MATLAB/Simulink, we applied Park's transformation, which allowed us to express the equations in a more manageable form. The obtained simulation results were then analyzed and interpreted to gain insights into the system's behavior.

One of the key observations was that the insertion of a load leads to speed variations, highlighting the strong coupling between the d-q axes. This coupling makes it challenging to control the two axes independently using conventional methods. To overcome this issue, the vector control technique based on flux orientation, will introduced in the next chapter. This approach allows for independent adjustment of each axis, thereby improving the precision and efficiency of the motor control strategy.

CHAPTER 3

Sliding Mode Controlof The Six-PhaseInduction Machine

3.1. Introduction :

In the domain of the electrical machine command, the oriental search engine, more and more, includes the application of modern command techniques. These techniques develop a digital way with the development of numerical calculations and electronic devices. This allows you to access the industrial processes of performances. This technique is better for one class participle of the command for one application given, depending on the form of the system's équations and such but environmentally friendly. We also call the example, the command by the flow logic, the adaptive command and the command with variable structure (CSV) that, in the electronic generation bibliographie, port the name of the command in sliding mode. The commands with variable structure are known to be robot commands in relation to parametric variations and are not very demanding in terms of computation time de calcul. The current connection to this one is due to the vulnerability of interruptors to the frequency of communication highs and more microprocessors and more performants [SAD17].

In effect, this is not part of the fourth anniversary (1980), challenges due to a major revolution in the domains of information and electronic devices, that the variable structure command in a sliding mode is developed in an interesting and attractive way. It is considered as one of the most simple approches for the command of non-linear systems and the systems tha thave a different model. This type can control incontestable advances, tell you that the robustness of the parameters, the implantation failure and the capacity to restore perturbations [KEN12]. This strategy is used to apply to the machine asynchronously with the watch cap by [EME67] [UTK77]. The base of the command in sliding modes is forced to force the system, via a command that is discontinued to evoluater at different temperatures on a surface of the sliding.

The principauxinconvenients of this command type is the "chattering" phenomenon that is affected by the oscillations on the high frequency of the sliding surface. These "chattering" effects are limited when the part is discontinued by the log flow, in this case, on the option of a hybrid command that says the command in glissant flow mode [LAR17].

The command in the glissant flow mode is one of the powerful commands of the most valuable ones that consist of combining multiple techniques: flow logic and glissement mode for exploitation. The advantages of both techniques at the same time, in order to limit the.. Inconveniences of regulation by les algorithms of regulating classes and better performance of the system to the commander (stabilité, precision, rapidity, robustness, etc.) [LEK16].

.

3.2. System structure is variable :

A variable structure is a system that does not change the structure due to its function, it is affected by the choice of structure and the logic of communication. This allows the commuter system to connect to the entire structure immediately. Moreover, this system can use new properties that do not exist in the chaque structure [YAH11].

3.2.1. System representation:

A system is said to have variable structure if it admits a representation by differential equations of the type:

$$X^* = \begin{cases} F_1(X,t) & \text{if condition (1) is verified.} \\ F_n(X,t) & \text{if condition (n) is verified} \end{cases} \qquad (3.1)$$

Where X is the state vector and the functions Fi belong to a set of subsystems, and are called structures. Indeed, there are commutations between these different structures depending on the condition verified. The study of such systems is of great interest, particularly in physics, mechanics and electricity. This is due to the stability properties that the overall system can have independently of those of each subsystem.

3.2.2. Generalities on the theory of sliding mode control:

In variable structure systems using sliding mode control, three basic configurations can be found for the synthesis of the different controls. [LAA17]

3.2.2.1. Structure by switching at the control unit level:

The diagram of this structure is given in Figure 3.1 :

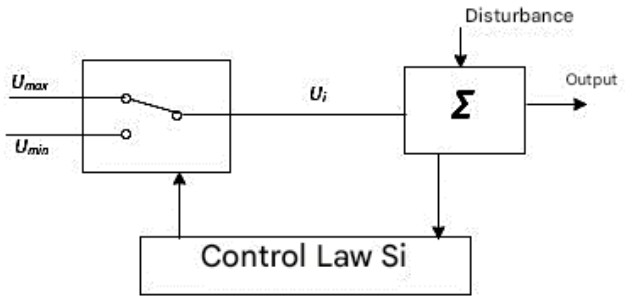

Figure 3.1 : *Switching regulation structure at the control unit level.* [LAA17]

This structure is simpler where the switching takes place at the level of the control unit itself. It corresponds to the operation (all or nothing) of the power switches associated in a large majority of applications with variable speed drives. It has been used for the control of stepper motors.

3.2.2.2. Switching structure at the state feedback level

The second structure involves switching at the level of a state feedback. Which relies on control by adjusting the dynamics of the system is achieved by gains or adjustments of classical state feedback. It has been implemented in the control of DC and permanent magnet motors, as well as in the control of induction machines..

We can see the diagram of this structure in figure:3.2 :

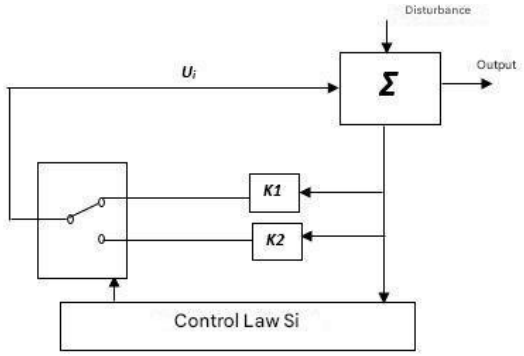

Figure 3.2 : *Switching regulation structure at the state feedback level.* [LEK16]:

IV.2.2.3. Structure by switching at the control organ level, with addition of the equivalent control:

The last structure is a switching structure at the control organ level with the addition of "equivalent control".

It allows the future state of the system to be pre-positioned using the equivalent control, which is nothing other than the desired value of the system in steady state. The control organ is much less stressed, the structure whose principle is shown in figure

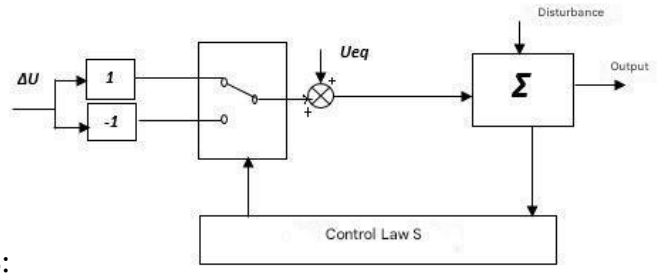

3.3:

Figure 3.3 : *Regulation structure by adding the equivalent command.* [LEK16]:

3.3. Principle of sliding mode control of variable structure systems:

The principle of sliding mode control consists of bringing the state trajectory of a system to a suitably selected region in a finite time. The region considered is then designated as a sliding or switching surface representing a relationship between the system's state variables. It is defined by a differential equation that completely determines the system's dynamics. The resulting dynamic

behavior is called the sliding regime. The system's behavior can be described by two phases [LEK16]:

- Convergence phase: This phase corresponds to the time interval during which the system's state trajectories are not on the sliding surface.
- Sliding phase: This phase corresponds to the time interval during which the state trajectories are confined within the sliding surface and the system's behavior no longer depends on the original system or disturbances, but is entirely determined by the sliding surface..

3.3.1 mode of a state. Trajectory variable:

In the control of variable structure systems with sliding mode, the state trajectory is brought towards a surface (hyperplane) and then, using the commutation law, it is forced to remain in the vicinity of this surface. The latter is called the sliding surface..

The trajectory in the phase plane consists of three distinct parts (figure 3.4) :

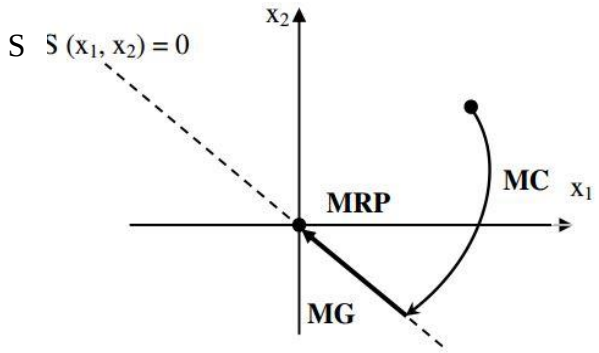

Figure 3.4 :*different modes for the trajectory in the phase plane.* .[LEK16].

Convergence mode (CM): this is the mode in which the variable to be controlled moves from any initial point in the phase plane and tends towards the switching surface S(x1, x2) = 0. This mode is characterized by the control law and the convergence criterion.

Sliding mode (MG): this is the mode during which the state variable has reached the sliding surface and tends towards the origin of the phase plane. The dynamics of this mode is characterized by the choice of the sliding surface$S(x_1, x_2)$.

Steady State Mode (SSM): This mode is added for the study of the system response around its equilibrium point, it is characterized by the quality and performance of the control.

3.3.2. Conditions for the existence of sliding mode:

The sliding mode exists when the switching takes place continuously between Umax and Umin, this phenomenon is illustrated in figure 3.5, for the case of a second-order adjustment system with the two state quantities xS1 and xS2 [LAA14]

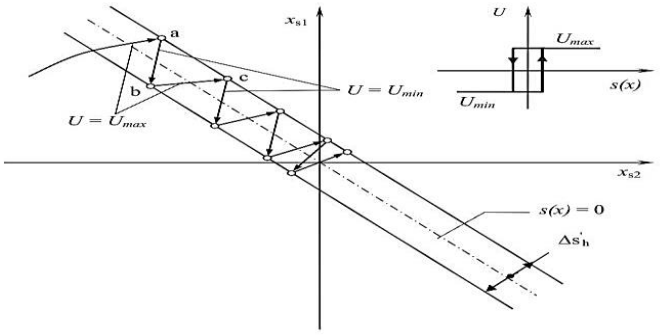

.

Figure 3.5 : *State trajectory in sliding regime.*[SAD17].

We first admit a hysteresis on the commutation law $s(x) = 0$ (dash line) the parallel offset lines of $\pm\Delta s'_h$[SAD17].

A trajectory with $U = U_{max}$touches the lower tipping threshold at point "a". If with

$U = U_{min}$the trajectory is oriented towards the inside of the hysteresis zone, it touches at point "b" the upper switching threshold where a switching takes place on $U = U_{max}$.

If the trajectory is oriented inward again, it touches the lower switching threshold at point "c" and so on. There is therefore a continuous movement within the hysteresis zone.

This movement approaches the steady state in a certain zone where continuous switching exists, the switching frequency is finite [LAA14].

3.4. Design of the sliding mode control:

The design of sliding-mode controllers systematically addresses stability and performance issues. It is often preferable to specify the system dynamics during convergence mode. In this case, the controller structure consists of two parts:

A continuous part, representing the system dynamics during sliding mode. And a discontinuous part, representing the system dynamics during convergence mode. This second part is important in nonlinear control because it eliminates the effects of inaccuracy and perturbations on the model [SAD17].

Implementing this control method requires three main steps:

1. Choosing the surface.

2. Establishing the conditions for convergence.

3. Determining the control law.

3.4.1. Choice of sliding surface:

The sliding surface is generally written as a function of the output's deviation from its desired value. The objective of the control is to ensure the tracking of a reference signal such that the deviation "e" tends to zero. The choice of the sliding surface concerns not only the required number of these surfaces, but also their shape. These two factors depend on the application and the desired objective.

For a system defined by the following state model, the surface vector has the same dimension as the control vector *u*.

$$[\dot{x}] = [A][x] + [B][u] \qquad (3.2)$$

Or Où $[x] \in \mathbb{R}^n$ is the state vector, $[x] \in \mathbb{R}^m$ the control vector, with n > m generally.

Regarding the shape of the surface, J.J. Slotine proposes a general equation form to determine the sliding surface that ensures the convergence of a state

x_i vers sa valeur de consigne $x_{i\,ref}$.

The general form is:

$$s_i(x_i) = \left(\frac{d}{dt} + \lambda_i\right)^{r-1}.e_i(x_i)/i = 1\ldots m \qquad (3.3)$$

with :

$e_i(x)$: The gap on the variables to be adjusted $e_i(x) = x_i - x_{iref}$;

λ_i : Positive constant vector that interprets the bandwidth of the desired control ;

r : Relative degree, equal to the number of times the output must be derived to make the command appear.

For : $r = 1$ $\quad s(x) = e(x)$

For : $r = 2$ $\quad s(x) = \lambda_x e(x) + \dot{e}(x)$

For: $r = 3$ $\quad s(x) = \lambda_x^2 e(x) + 2\lambda_x \dot{e}(x) + \ddot{e}(x)$

The objective of the command is to keep the surface s(x) equal to zero. The latter

is a linear differential equation whose unique solution is $e(x) = 0$, for a suitable choice of the parameter λ_i.

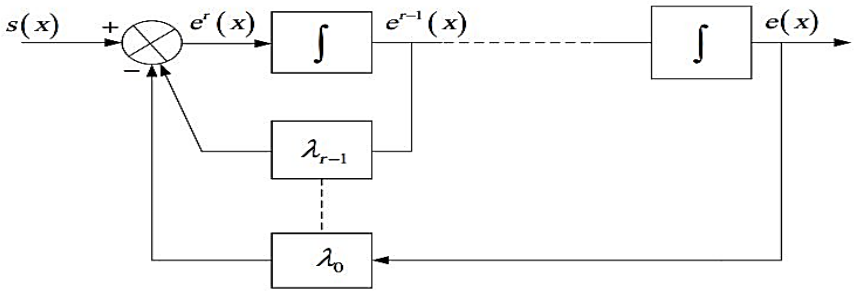

Figure 3.6 :*Exact linearization of the deviation.* [SAD17].

3.4.2. Conditions of existence and convergence of the sliding regime:

The conditions of existence and convergence are the criteria that allow the different dynamics of the system to converge towards the sliding surface and to remain there independently of the disturbance. We present two types of conditions which are [YAH11].

3.4.2.1. Direct approach:

This approach is the oldest, it is proposed and studied by Emilyanov and Utkin. It is given in the form.

$$s(x).\dot{s}(x) < 0. \tag{3.4}$$

3.4.2.2. Lyapunov's approach:

This involves formulating a positive scalar function v(x) > 0 for the system's state variables and choosing a control law that will cause this function to decrease $\dot{v} < 0$ and used to estimate control performance such as the study of the robustness of nonlinear systems.

For example, by defining a candidate Lyapunov function for the system as follows :

$$v(x) = \frac{1}{2}s^2(x) \tag{3.5}$$

By deriving the latter, we obtain:

$$\dot{v}(x) = s(x)\dot{s}(x) \tag{3.6}$$

For the Lyapunov candidate function to decrease, it is sufficient to ensure que :

$$s(x).\dot{s}(x) < 0. \tag{3.7}$$

3.4.3. Determination of the control law:

Once the sliding surface and the convergence criterion have been chosen, it remains to determine the command required to land the variable to be controlled towards the surface and then towards its equilibrium point while maintaining the condition of existence of sliding modes [LAZ17].The structure of the command has two parts, the first concerning the exact

linearizationU_{eq}, and a second stabilizer U_nThe latter is very important in sliding mode control technique, as it is used to eliminate model inaccuracy effects and reject external disturbances [AMM17].

$$U(t) = U_n + U_{eq} \tag{3.8}$$

U_{eq} : Corresponds to the equivalent command proposed by Filipov and Utkin, it is used to maintain the variable to be controlled on the sliding surface s(t).

U_n : is determined to verify the convergence condition.

Ueq can be considered as the continuous average value that the control takes during a rapid switching between two values Umin and Umax. Figure (3.7) corresponds to the control that guarantees the attractiveness of the variable to be controlled towards the surface and satisfies the condition: s(x).s ̇(x)<0 [LAR17].

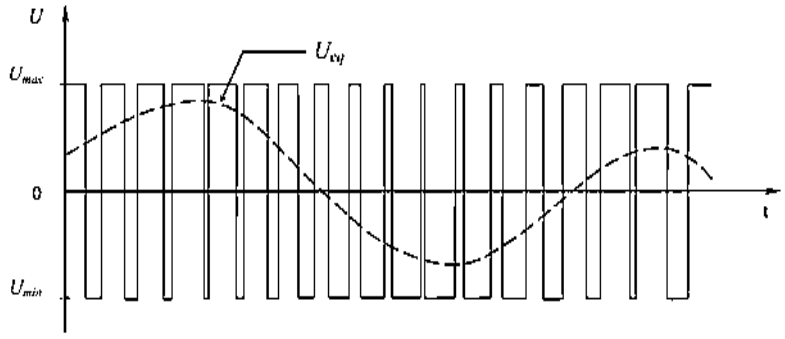

Figure 3.7 :*Equivalent and actual order.* [LAR17].

In order to highlight the previous development, we consider the state system (3.2). We seek to determine the analogical expression of the U command. The derivative of the surface s (*x*) is :

$$\dot{s}(x) = \frac{ds}{dt} = \frac{\partial s}{\partial x}.\frac{\partial x}{\partial t} \tag{3.9}$$

Substituting (3.2) and (3.8) into (3.9), we find:

$$\dot{s}(x) = \frac{ds}{dt} = \frac{\partial s}{\partial x}\{[A][x] + [B]U_{eq}\} + \frac{\partial s}{\partial x}[B]U_n \tag{3.10}$$

During the sliding mode and the steady state, the surface is zero and therefore, its derivative and the discontinuous part are also zero (Un = 0). From this, we deduce the expression of the equivalent control:

$$U_{eq} = -\{\frac{\partial s}{\partial x}[B]\}^{-1}\{\frac{\partial s}{\partial x}[A][x]\} \tag{3.11}$$

For the equivalent order to take a finite value, it is necessary that:

$$\frac{\partial s}{\partial x}[B] \neq 0 \tag{3.12}$$

During the convergence mode and replacing the equivalent command by its expression in (3.10), we obtain the new expression for the derivative of the surface:

$$\dot{s}(x) = \frac{\partial s}{\partial x}[B]U_n < 0 \qquad (3.13)$$

With the attractiveness condition s(x).s ̇(x)<0, we obtain:

$$s(x)\frac{\partial s}{\partial x}[B]U_n < 0 \qquad (3.14)$$

In order to satisfy the condition, the sign of One must be opposite to that de $s(x)\frac{\partial s}{\partial x}[B]$.

The simplest form that discrete control can take is that of a sign function (figure 3.8)

:$U_n = K_x sign S(x)$ (3.15)

The sign of Kx must be different from that of $\frac{\partial s}{\partial x}[B]$.

Where: Sign (S(x)) is the function defined by [66]:

$$sign\big(S(x)\big) = \begin{cases} -1 & si \quad S(x) < 0 \\ 1 & si \quad S(x) > 0 \end{cases} \qquad (3.16)$$

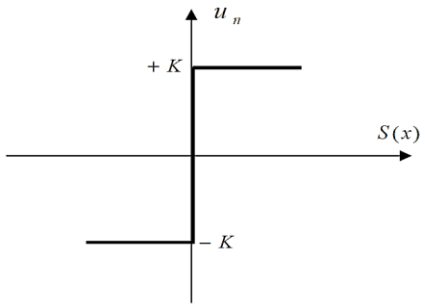

Figure 3.8 : *: Sign function (Relay type control).* [SAD17].

Using the "Sign" function means that the command between two values ± K with a theoretically infinite frequency if the gain K is very small. The response time will be long if the gain K is very large, otherwise the rethinking time will be fast but unwanted oscillations may appear "Commonly called Chattering" on the steady-state responses. In order to reduce high-frequency oscillations (undesirable on the responses), classic solutions consist of imposing a variation of the command value according to the distance between the state variable and the sliding surface. However, it is possible to eliminate this phenomenon by introducing a layer boundary around the sliding surface (S = 0) with a threshold 2φ, , the following figure represents the boundary layer in sliding mode [SAD17].

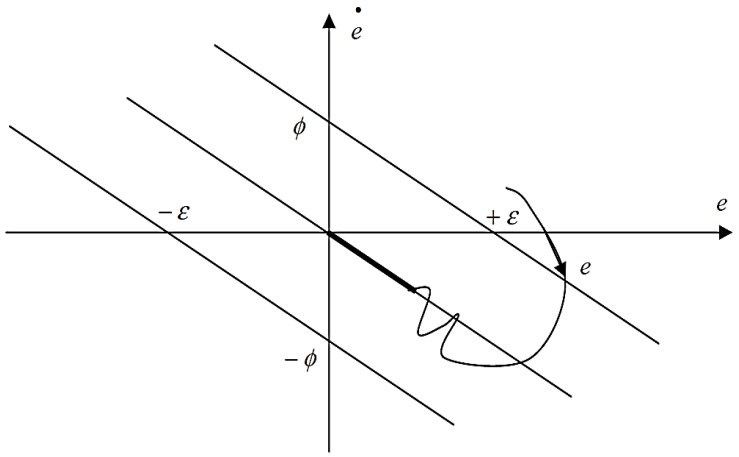

Figure 3.9 : *Sliding mode with a boundary layer.* [LAZ18]:

Then state 'e' is in the boundary layer if: $S< \varphi$.

If the boundary layer is incorporated into the order, we obtain:

$$U_n = K.F_{sat}\left(\frac{S}{\varphi}\right) \tag{3.17}$$

F_{sat} : the saturation function, it is defined as follows:

$$F_{sat}\left(\frac{S}{\varphi}\right) = \begin{cases} \frac{S}{\varphi} & si \quad \left|\frac{S}{\varphi}\right| < 1 \\ sign\left(\frac{S}{\varphi}\right) & si \quad \left|\frac{S}{\varphi}\right| > 1 \end{cases} \tag{3.18}$$

3.5. Determination of the different regulation surfaces and application:

The system of state equations is derived from the synthesis of control laws, which is based on the model obtained after decoupling by the vector control method [LAZ18]:

$$\begin{cases} i_{ds1}^{\bullet} = \frac{1}{L_{s1}}(v_{ds1}^{*} - L_{s1}i_{ds1} + \omega_s^{*}(L_{s1}i_{qs1} + T_r\varphi_r^{*}\omega_{gl}^{*})) \\ i_{qs1}^{\bullet} = \frac{1}{L_{s1}}\left(v_{qs1}^{*} - L_{s1}i_{qs1} - \omega_s^{*}(L_{s1}i_{ds1} + \varphi_r^{*})\right) \\ i_{ds2}^{\bullet} = \frac{1}{L_{s2}}(v_{ds2}^{*} - L_{s2}i_{ds2} + \omega_s^{*}(L_{s2}i_{qs2} + T_r\varphi_r^{*}\omega_{gl}^{*})) \\ i_{qs2}^{\bullet} = \frac{1}{L_{s2}}\left(v_{qs2}^{*} - L_{s2}i_{qs2} - \omega_s^{*}(L_{s2}i_{ds2} + \varphi_r^{*})\right) \\ \dot{\Omega} = \frac{1}{J}\left(p\frac{L_m}{L_m+L_r}(i_{qs1} + i_{qs2})\varphi_r{}^{*} - f.\Omega - C_r\right) \\ \dot{\varphi} = -\frac{R_r}{L_m+L_r}\varphi_r + \frac{R_r.L_m}{L_m+L_r}(i_{ds1} + i_{ds2}) \end{cases} \tag{3.19}$$

3.5.1. Speed control surface:

This variable is the speed, so we choose a surface of order 1 which is enough to make the command appear:

$$s(\omega_r) = \omega_r^{*} - \omega_r \tag{3.20}$$

with : $$\Omega = \omega_r/p \tag{3.21}$$

The derivative of the surface is given by:

$$\dot{s}(\omega_r) = \dot{\omega}_r^* - \dot{\omega}_r \quad (3.22)$$

From equation number (5) of the system of equation (3.19) becomes:

$$\dot{\omega}_r = \frac{p^2}{J}\frac{L_m}{L_m+L_r}(i_{qs1} + i_{qs2})\varphi_r^* - \frac{f}{J}\omega_r - \frac{p}{J}C_r \quad (3.23)$$

By posing: $i_{qs1} + i_{qs2} = i_{qs}$ (3.24)

SO : $\dot{\omega}_r = \frac{p^2}{J}\frac{L_m}{L_m+L_r} i_{qs}\varphi_r^* - \frac{f}{J}\omega_r - \frac{p}{J}C_r$ (3.25)

Now, replacing the iqs current with the control current $i_{qs}^* = i_{qseq} + i_{qsn}$ in equation (3.23), we find:

$$S(\dot{\omega}_r) = \dot{\omega}_r^* - \frac{p^2}{J}\frac{L_m}{L_m+L_r} i_{qseq}\varphi_r^* - \frac{p^2}{J}\frac{L_m}{L_m+L_r} i_{qsn}\varphi_r^* - \frac{f}{J}\omega_r - \frac{p}{J}C_r \quad (3.26)$$

During sliding mode and steady state, we have $s(\omega_r)=0$ and consequently $\dot{s}(\omega_r) = 0$et $i_{qsn}=0$ d' where we have:

$$i_{qseq} = \frac{J}{p^2}\frac{L_m+L_r}{L_m.\phi_r^*}\left[\dot{\omega}_r^* + \frac{f}{J}\omega_r + \frac{p}{J}C_r\right] \quad (3.27)$$

During the convergence mode, the condition $s(x).\dot{s}(x) < 0$must be verified. Replacing (3.26) and (3.27) we have [LAZ18]:

$$\dot{s}(\omega_r) = -\frac{p^2}{J}\frac{L_m\varphi_r^*}{L_m+L_r}.i_{sqn} \quad (3.28)$$

We take: $i_{qsn} = K_{\omega_r}\frac{s(\omega_r)}{|s(\omega_r)|+\xi_{\omega_r}}$ (3.29)

3.5.2. Rotor flux control surface:

Taking the same area as that of the speed:

$$s(\varphi_r) = \varphi_r^* - \varphi_r \quad (3.30)$$

$$\dot{s}(\varphi_r) = \dot{\varphi}_r^* - \dot{\varphi}_r \quad (3.31)$$

By posing: $i_{ds1}+i_{ds2}=i_{ds}$, and substituting the equation of φ_r^• into equation 4.31 :

$$\dot{s}(\varphi_r) = \dot{\varphi}_r^* + \frac{R_r}{L_m+L_r}\varphi_r - \frac{R_r.L_m}{L_m+L_r} i_{ds} \quad (3.32)$$

Now, replacing the current $i_{ds}$by the control current $i_{dseq} + i_{dsn} = i_{ds}^*$ in equation (3.32), we find:

$$\dot{s}(\varphi_r) = \dot{\varphi}_r^* + \frac{R_r}{L_m+L_r}\varphi_r - \frac{R_r.L_m}{L_m+L_r} i_{dseq} - \frac{R_r.L_m}{L_m+L_r} i_{dsn} \quad (3.33)$$

During sliding mode and steady state, we have $s(\varphi_r) = 0$ and consequently $\dot{s}(\varphi_r) = 0$ and $i_{dsn}= 0$ from where we have:

$$i_{dseq} = \frac{L_m+L_r}{L_m.R_r}\left[\dot{\varphi}_r^* + \frac{L_m.\varphi_r}{L_m+L_r}\right] \quad (3.34)$$

During convergence mode, the condition $s(x).\dot{s}(x) < 0$must be checked. By replacing (4.33) and (4.34) we have [LAZ18] :

$$\dot{s}(\varphi_r) = -\frac{R_r.L_m}{L_m+L_r} i_{sdn} \tag{3.35}$$

We take: $i_{dsn} = K_{\varphi_r} \frac{s(\varphi_r)}{|s(\varphi_r)|+\xi_{\varphi_r}}$ (3.36)

3.5.3. Stator current regulation surface:

We take the following surfaces:

$$\begin{cases} s(i_{ds1}) = i_{ds1}^* - i_{ds1} \\ s(i_{qs1}) = i_{qs1}^* - i_{qs1} \\ s(i_{ds2}) = i_{ds2}^* - i_{ds2} \\ s(i_{qs2}) = i_{qs2}^* - i_{qs2} \end{cases} \tag{3.37}$$

The derivatives of these are respectively:

$$\begin{cases} \dot{s}(i_{ds1}) = \dot{i}_{ds1}^* - \dot{i}_{ds1} \\ \dot{s}(i_{qs1}) = \dot{i}_{qs1}^* - \dot{i}_{qs1} \\ \dot{s}(i_{ds2}) = \dot{i}_{ds2}^* - \dot{i}_{ds2} \\ \dot{s}(i_{qs2}) = \dot{i}_{qs2}^* - \dot{i}_{qs2} \end{cases} \tag{3.38}$$

We replace the currents : $\dot{i}_{ds1}, \dot{i}_{qs1}, \dot{i}_{ds2}, \dot{i}_{qs2}$of equation (3.38) by their expressions given in the system of equations (3.19), we will have:

$$\begin{cases} \dot{s}(i_{ds1}) = \dot{\imath}_{ds1}^* - \frac{1}{L_{s1}}\left(v_{ds1} - R_{s1} i_{ds1} + \omega_s^*\left(L_{s1} i_{qs1} + T_r \varphi_r^* \omega_{gl}^*\right)\right) \\ \dot{s}\left(i_{qs1}\right) = \dot{\imath}_{qs1}^* \frac{1}{L_{s1}}\left(v_{qs1} - R_{s1} i_{qs1} - \omega_s^*\left(L_{s1} i_{ds1} + \varphi_r^*\right)\right) \\ \dot{s}(i_{ds2}) = \dot{\imath}_{ds2}^* - \frac{1}{L_{s2}}\left(v_{ds2} - R_{s2} i_{ds2} + \omega_s^*\left(L_{s2} i_{qs2} + T_r \varphi_r^* \omega_{gl}^*\right)\right) \\ \dot{s}\left(i_{qs2}\right) = \dot{\imath}_{qs2}^* \frac{1}{L_{s2}}\left(v_{qs2} - R_{s2} i_{qs2} - \omega_s^*\left(L_{s2} i_{ds2} + \varphi_r^*\right)\right) \end{cases} \tag{3.39}$$

By replacing the voltages vds1, vqs1, vds2, vqs2 with the control voltages $\dot{v_{ds1}}, \dot{v_{qs1}}, \dot{v_{ds2}}, \dot{v_{qs2}}$d'où :

$$\begin{cases} v_{ds1}^* = v_{ds1eq} + v_{ds1n} \\ v_{qs1}^* = v_{qs1eq} + v_{qs1n} \\ v_{ds2}^* = v_{ds2eq} + v_{ds2n} \\ v_{qs2}^* = v_{qs2eq} + v_{qs2n} \end{cases} \tag{3.40}$$

We will have:

$$\begin{cases} \dot{s}(i_{ds1}) = i_{ds1}^{*\cdot} - \frac{1}{L_{s1}}\left(-R_{s1}i_{ds1} + \omega_s^*\left(L_{s1}i_{qs1} + T_r\varphi_r^*\omega_{gl}^*\right) + v_{ds1eq} + v_{ds1n}\right) \\ \dot{s}(i_{qs1}) = i_{qs1}^{*\cdot}\frac{1}{L_{s1}}(-R_{s1}i_{qs1} - \omega_s^*(L_{s1}i_{ds1} + \varphi_r^*) + v_{qs1eq} + v_{qs1n})) \\ \dot{s}(i_{ds2}) = i_{ds2}^{*\cdot} - \frac{1}{L_{s2}}\left(-R_{s2}i_{ds2} + \omega_s^*\left(L_{s2}i_{qs2} + T_r\varphi_r^*\omega_{gl}^*\right) + v_{ds2eq} + v_{ds2n}\right) \\ \dot{s}(i_{qs2}) = i_{qs2}^{*\cdot}\frac{1}{L_{s2}}(-R_{s2}i_{qs2} - \omega_s^*(L_{s2}i_{ds2} + \varphi_r^*) + v_{qs2eq} + v_{qs2n})) \end{cases} \quad (3.41)$$

During sliding mode and steady state, we have $s(i_{ds1})=0$, $s(i_{qs1})=0$, $s(i_{ds2})=0$, $s(i_{qs2})=0$ and by suit$\dot{s}(i_{ds1})=0$, $V_{ds1n}=0$, $\dot{s}(i_{qs1})=0$, $V_{qs1n}=0$, $\dot{s}(i_{ds2})=0$, $V_{ds2n}=0$, $\dot{s}(i_{qs2})=0$, $V_{qs2n}=0$, alors on a:

$$\begin{cases} v_{ds1eq} = L_{s1}i_{ds1}^{*\cdot} - R_{s1}i_{ds1} + \omega_s^*(L_{s1}i_{qs1} + T_r\varphi_r^*\omega_{gl}^*) \\ v_{qs1eq} = L_{s1}i_{qs1}^{*\cdot} - R_{s1}i_{qs1} - \omega_s^*(L_{s1}i_{ds1} + \varphi_r^*) \\ v_{ds2eq} = L_{s2}i_{ds2}^{*\cdot} - R_{s2}i_{ds2} + \omega_s^*(L_{s2}i_{qs2} + T_r\varphi_r^*\omega_{gl}^*) \\ v_{qs2eq} = L_{s2}i_{qs2}^{*\cdot} - R_{s2}i_{qs2} - \omega_s^*(L_{s2}i_{ds2} + \varphi_r^*) \end{cases} \quad (3.42)$$

During the convergence mode, the condition$s(i_{ds1}).\dot{s}(i_{ds1}) < 0, s(i_{qs1}).\dot{s}(i_{qs1}) < 0$, $s(i_{ds2}).\dot{s}(i_{ds2}) < 0$, $s(i_{qs2}).\dot{s}(i_{qs2}) < 0$, must be checked. We have :

$$\begin{cases} \dot{s}(i_{ds1}) = -\frac{1}{L_1}v_{ds1n} \\ \dot{s}(i_{qs1}) = -\frac{1}{L_1}v_{qs1n} \\ \dot{s}(i_{ds2}) = -\frac{1}{L_2}v_{ds2n} \\ \dot{s}(i_{qs2}) = -\frac{1}{L_2}v_{qs2n} \end{cases} \quad (3.43)$$

We take respectively:

$$\begin{cases} v_{ds1n} = K_{d1}\frac{s(i_{ds1})}{|s(i_{ds1})|+\xi_{ds1}} \\ v_{qs1n} = K_{d1}\frac{s(i_{q1}s)}{|s(i_{qs1})|+\xi_{qs1}} \\ v_{ds2n} = K_{d2}\frac{s(i_{ds2})}{|s(i_{ds2})|+\xi_{ds2}} \\ v_{qs2n} = K_{q2}\frac{s(i_{qs2})}{|s(i_{qs2})|+\xi_{qs2}} \end{cases} \quad (3.44)$$

3.6. Applying the command by sliding mode:

The application of cascade adjustment of rotor speed and flux by sliding mode on the 6PH-IM with the direct method is illustrated by figure (3.10) [BEN18]:

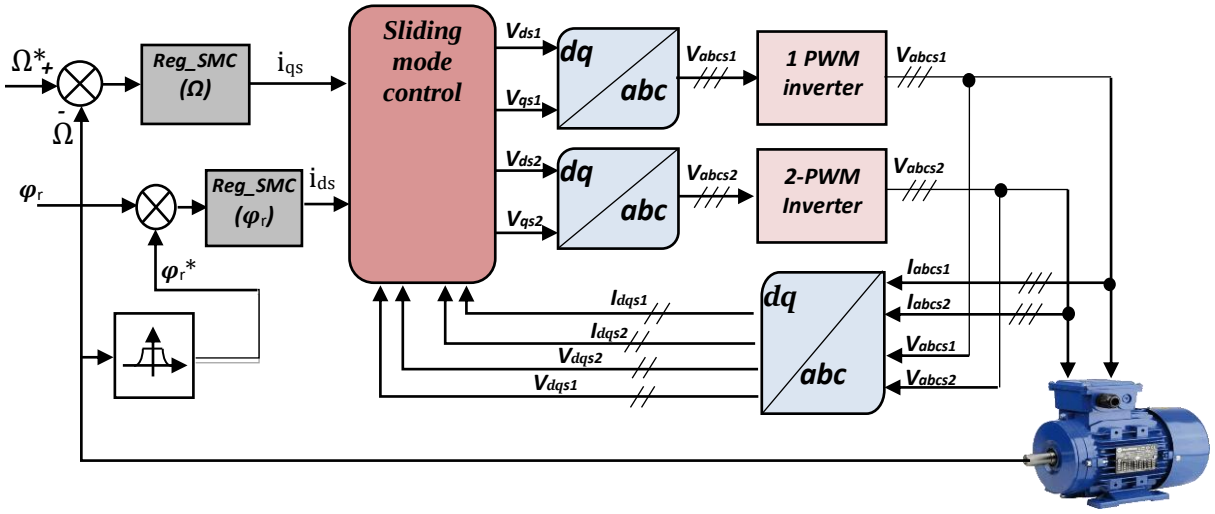

Figure 3.10 : *Block diagram for adjusting rotor speed and flux by sliding mode.* [BEN18]:

The diagram of the sliding mode control block is represented by the figure (Fig.IV.10), knowing that:

$i_{qs1}^{*} = i_{qs2}^{*}$ et $i_{ds1}^{*} = i_{ds2}^{*}$

The parameters of the different regulators by sliding mode are given in Table 3.1.

Surfaces	$s(\omega_r)$	$s(\phi_r)$	$s(i_{ds1})$	$s(i_{qs1})$	$s(i_{ds2})$	$s(i_{qs2})$
K	K=2000	K=180	K=400	K=400	K=400	K=400
ξ	ξ =0.05	ξ=0.06	ξ=0.001	ξ=0.001	ξ=0.001	ξ=0.001

Tableau 3.1 : *Settings of sliding mode controllers.*

IV.3 Simulation results for neural network-based vector control:

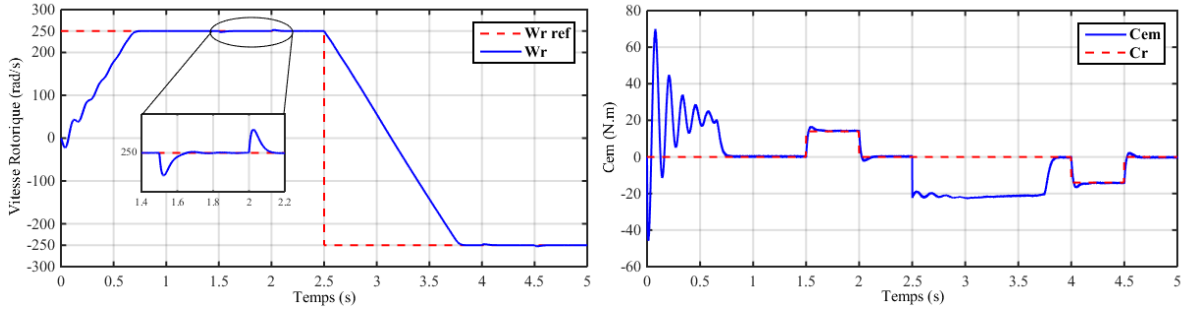

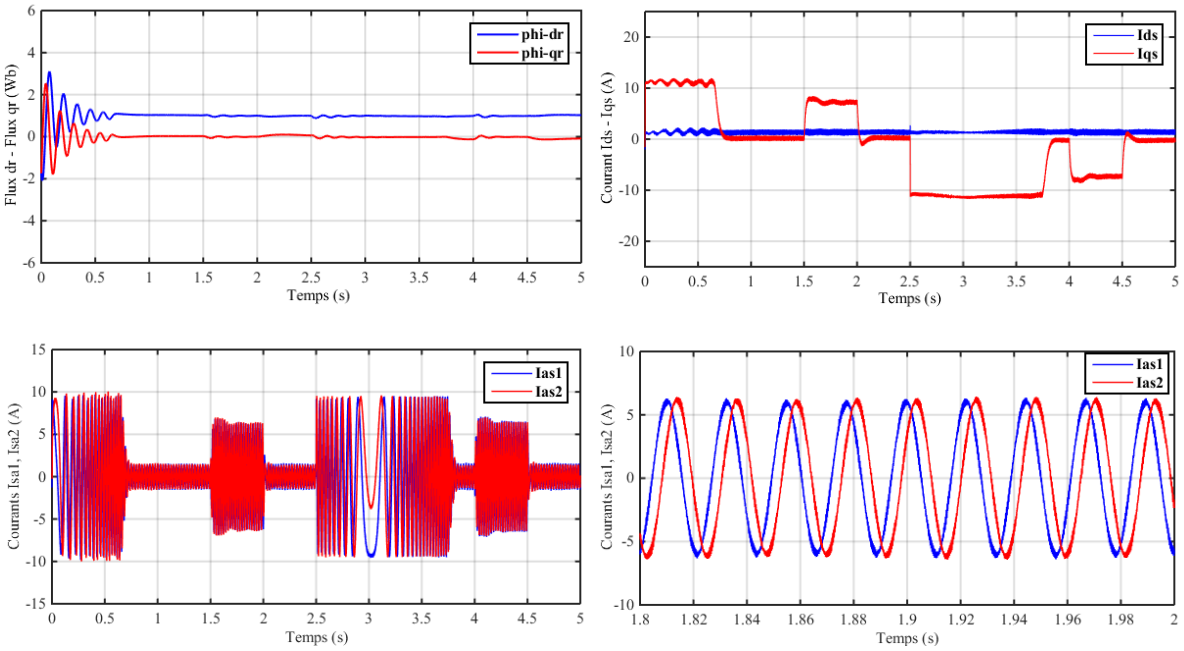

Figure 3.11 Evolution of 6PH-IM characteristics during neural network-based vector control.

Figure 3.11, shows the evolution of the neural network-based vector control characteristics applied to the D3P-IM, followed by speed inversion from 300 to -300 from time t = 2.5s and application of loads Cr = 14 Nm in time interval t = [1.5 ; 2] s

and Cr = -14Nm in t =[4 ; 4.5]s.

At start-up and during transient operation, speed increases linearly with time, reaching its reference value at t = 0.6s without overshooting. The electromagnetic torque reaches its maximum value at start-up, then reaches steady state at t = 0.6s. Initially, the stator current ias1 reaches an inrush current of around 10A. The quadrature current initially reaches 11A, after which it evolves identically to the electromagnetic torque. The rotor fluxes according to (d, q) show peaks for a fraction of a second at start-up, oscillating around their set points.

After t = 2.5s, the speed reverses and reaches its negative setpoint after t = 1.2s, with no overshoot. This generates an increase in the ias1 current of a magnitude equal to that recorded during start-up, which stabilizes after 1.2s to give rise to the steady-state form.

The electromagnetic torque reaches its maximum value at the moment of speed reversal, which stabilizes as soon as the speed reaches its reference value (-300 rad/s), the quadrature current iqs1 increases in a similar way to the electromagnetic torque, and the rotor fluxes along the axes (d, q) follow their reference values during speed reversal.

- **Robustness tests :**

In order to test the robustness of the sliding mode control, two tests are carried out. The first test is for the variation of the rotor resistance, the second test for the variation of the stator resistance.

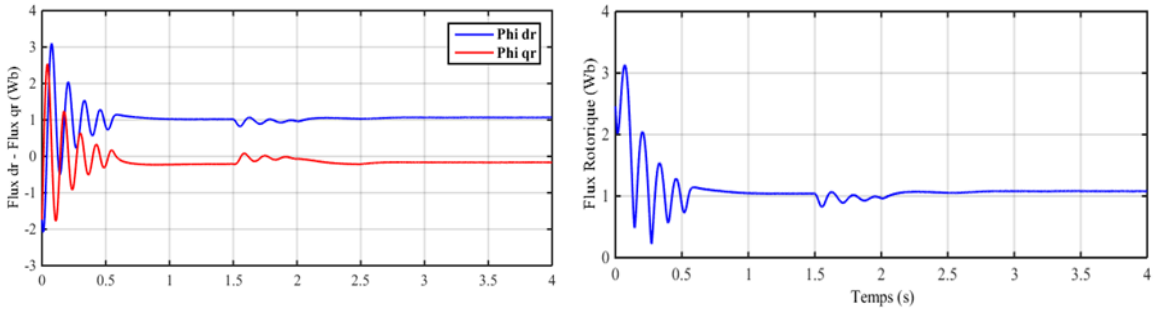

Figure 3.12 Robustness test for a +50% variation in rotor resistance, for 6PH-IM speed control (under nominal load) by sliding mode control.

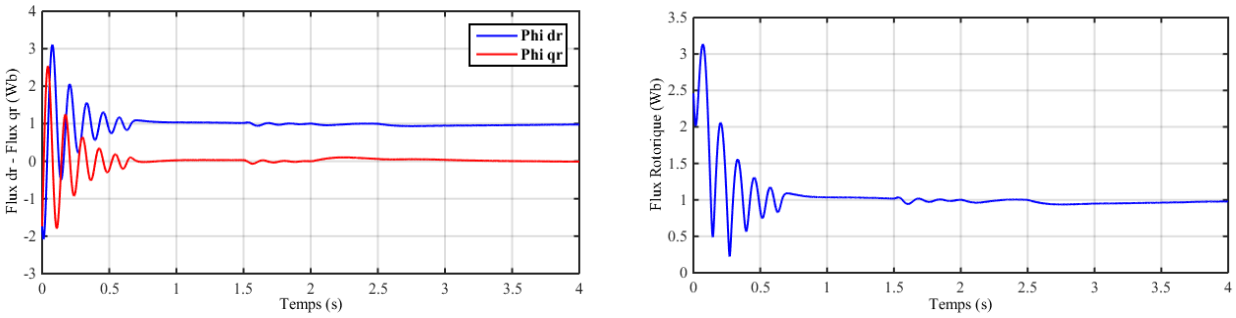

Figure 3.13 Robustness test for a +50% variation in stator resistance, for speed control of the 6PH-IM (under nominal load) by neural network-based vector control.

Figure 3.12 shows the evolution of 6PH-IM characteristics with sliding mode control, followed by a 50% increase in rotor resistance at time t = 2.5s with the application of loads Cr= 14N.m in the time interval t = [1.5 ; 2]s, while imposing the reference speed ωr*=300rad/s.

We note that a slight disturbance is observed by the rotor fluxes, which is due to the simultaneous effect of the variation in rotor resistance and load (Cr = 14N.m), as from t = 2.5s they resume their progressions according to their set points without disturbance.

Figure 3.13 shows the evolution of 6PH-IM characteristics with sliding mode control, followed by the 50% increase in stator resistance at time t = 2.5s with the application of Cr=14N.m loads in the time interval t = [1.5; 2]s, while imposing reference speed ωr*=300rad/s.

Simulation results clearly show the robustness of the sliding mode control to variations in stator and rotor resistances.

3.7 Conclusion

This chapter focuses on implementing sliding mode control for the 6PH-IM, with the primary goal being speed regulation. Initially, a theoretical overview of sliding mode control in variable structure systems was presented. This was followed by a detailed explanation of the steps involved in designing the control algorithm, which was then applied to the 6PH-IM. Finally, the simulation results were shown and analyzed.The speed regulation through sliding mode control demonstrated faster responses in the absence of load and more robust performance when the load varied, regardless of the studied operating conditions. The tests, which involved reversing the speed and varying the resistance under full load conditions, clearly indicated that the system was unaffected by the first test and only slightly sensitive to the combined effect of rotor resistance changes and load application from these observations, it is concluded that sliding mode control significantly enhances speed regulation compared to traditional algorithms. these controllers offer superior static and dynamic performance (such as stability and precision), with quicker response times, no overshoot, better tracking, and near-total disturbance rejection.

General Conclusion

General Conclusion

The work presented in this thesis exposes the synthesis of a reliable and high-quality control technique, for the speed regulation of a six-phase induction machine (6PH-IM), once by vector control based on two-level converters and another time based on multi-level converters. The main objective of this thesis is to improve the control performance in terms of quality, reliability and accuracy. This study was made in three chapters:

In the first chapter, we examined the six phase machines and their properties, and discovered that they are the typical example of these machines. In which, the six phase machine offers a good technical and economic compromise for high energy applications such as pumps, fan, cement plants etc.

In Chapter II, our efforts were dedicated to the modeling of the six-phase induction machine, the model that describes the equations of 6PH-IM was developed in the vertical and horizontal axis system thanks to the Park conversion matrix. Remember that the study was conducted at a shift angle of 30 degrees between the two stars.

In the last chapter, the sliding mode control of the six-phase induction machine, whose principle is to have a torque similar to that of the DC device. To do this, we base on the indirect rotor flow guideline that is applied to control speed, and then the device is attached to two voltage converters controlled by the PWM pulse width modulation technology, which produces torque harmonies while maintaining robustness and performance compared to traditional techniques.

After consulting the obtained results from chapter three, it is possible to envisage interesting perspectives and practical developments that could help to exploit this machine better:

- Using multi-level converters topologies;

- Application of other robust control techniques, such as fuzzy logic, predictive control, neural networks, genetic algorithms, etc.

-Finally, experimental validation in real time of the proposed methods.

REFERENCES

REFERENCES

[BER16] BERRABAH Fouad,« Commande Sans Capteur De La Machine Asynchrone », Thèse De Doctorat De l'Université BADJI MOKHTAR – ANNABA, 2016

[RAH20] RAHAL HILAL, « Commande non Linéaires Hybrides et roboustes de la Machine Asynchrone Double Etoile», Théses de Doctorat,Université Mohamed BOUDIAF De MSILA 2020

[HAD01] D. Hadiouche, « contribution à l'étude de la machine asynchrone double étoile : modélisation, alimentation et structure», Thèse de doctorat de Université Henri Poincaré, Nancy-1., soutenue 20 décembre 2001

[AMI08] H.AMIMEUR, « Contribution à la Commande d'une Machine Asynchrone Double Etoile par Mode de Glissement »,Mémoire De Magister, Université El Hadj Lakhdar de Batna, 2008

[MES22] Mesai Ahmed Hamza « Commandes de hautes Performances d'une Machine Asynchrone Double Etoile MASDE via des Convertisseurs Multi-niveaux » Thesis Doctorat, Université DJILLALI LIABES De SIDI-BEL-ABBES, 2022.

[BOS09] B. K. Bose, "Power electronics and motor drives recent progress and perspective," IEEE Trans. Ind. Electron., vol. 56, no. 2, pp. 581–588, Feb. 2009

[AMI12]H.AMIMEUR,« Contribution ou Control de la Machine Asynchrone Double Etoile »,Thése Doctorat, Université El Hadj Lakhdar de Batna, 2012.

[ABA22] W.ABADI and **H.GABOUSSA** and **C.E.SOUSSA** and **A.HECHIFA,** « Commande Par Mode Glissant de la Machine Double Etoile » Mémoire Master académique, Université EchahidHamma Lakhdar d'El-oued,2022.

[DJA13]A.DJABOREI « Etude Commande de la Machine Asynchrone Double Etoile » Mémoire de Master académique,Université KasdiMerbah de Ouargla, 2013.

[Zahr 17] A. K. Abdul Zahra, "Robust Control of Vehicle Suspension Systems Using Sliding Mode Control," University of Basrah, 2017.

[Maj20] H. S. Majid, "Design and Control of an Artificial Finger Using Sliding Mode Technique," University of Technology, Iraq, 2020.

[Maa19] F. Maallem, M. Maallem, "Landslide Risk Assessment in Constantine: Structural and Urban Implications," University of Mohamed Boudiaf, 2019.

[Utk93] V. Utkin, "Sliding Mode Control Design Principles and Applications to Electric Drives," IEEE Transactions on Industrial Electronics, vol. 40, no. 1, pp. 23–36, 1993.

[Sht12] Y. Shtessel, C. Edwards, L. Fridman, and A. Levant, Sliding Mode Control and Observation, Springer, 2012.

[Edw00] C. Edwards and S. K. Spurgeon, Sliding Mode Control: Theory and Applications, Taylor & Francis, 2000.

[Arz–] D. Arzelier, D. Peaucelle, Syst`emes et asservissement non lin´eaires, Notes de Cours, Version 4, CNAM–B2.

[MESS18] Z.M.N.ZOUAOUID and **M.T.MESSAI**, « Commande Vectorielle de la Machine à Double Stator », Mémoire Master, Université Larbi Ben M'Hidi Oum EL Bouaghi, 2018.

[RAZ00]D.Hadiouche and**H.Razik** and**A.Rezzoug,** « Modelling of a double-star induction motor with an arbitrary shift angle between its three phase windings » , EPE-PEMC2000, Kosice

[KER13] KERCHA SAFIA GOUBI WISSAM Etude et modélisation des machines électriques double étoile **Soutenu publiquement** Le :27/06/2013 UNIVERSITÉ KASDI MERBAH OUARGLA

[LOU14] Etude et Commande d'une Machine Asynchrone Double Etoile Mr Lounes HAMA Mr Mounir KEKOUCHE Promotion 2013-2014Université A.MIRA-BEJAIA

[OUA17] : Fouad OUKRID : Chafaa RABHI Commande d'un aérogenerateur basé sue une machine asynchrone double étoile2016/2017

[MOU99] Mobaid, N. (1999). Feeding by tension boosters for multi-star machines [Doctoral Institute, National Polytechnic Institute of Lorraine, Nancy, France

[KIY20] Y.KICHENE and **B.ZAOUALI,** «Commande Intelligante Floue d'une Machine Asynchrone Double Etoile » Mémoire présenté pour l'obtention Dudiplôme deMasterProfessionnel, Université Mohamed BOUDIAF De MSILA, 2020.

[EME67]S. V.E**melyanov**, "Variable structure control systems (in Russian)," Moscow, Nauka, 1967

[UTK77] V.I. UTKIN, "Variable structure systems with sliding modes : a survey. IEEE Trans. Autom. Control, vol. 22, no. 2, pp. 212–222, 1977.

[YAH11] A. YAHDOU, "Commande et observation par modes glissants d'une machine asynchrone double étoile sans capteur mécanique," Mémoire de Magister de l'université deChlef, Algérie, Avril 2011.

[48] T. LAAMAYAD, "Contribution à la Commande d'une Machine Asynchrone Double Etoile par Mode Glissant. Apport de la Logique floue," Thèse de Doctorat de l'université de Batna, Algérie, Octobre 2014.

[SAD 17] R. SADOUNI, "Commande directe du couple (DTC-SVM) d'une MASDE associéeà Deux Onduleurs Multiniveaux en Cascade avec un Redresseur à MLI Piloté par DPC," Thèse de Doctorat de l'université de Sidi Bel Abbes, Algérie, Octobre 2017.

[KEN12] K. KENDOUCI, "Contribution à la commande sans capteur mécanique d'une machine synchrone à aimants permanents," Thèse de Doctorat de l'Université des Sciences et de la Technologie d'Oran, Algérie, 2012.

[LAR17] A. LARBAOUI, B. BELABBES, A. MEROUFEL, D.BOUGUENNA, "Fuzzy sliding mode control for synchronous machine," Rev. Roum. Sci. Techn– Électrotechn and Énerg. vol. 62, no. 2, pp. 192–196, Bucarest, 2017.

[LEK16] S. LEKHCHINE, T. BAHI, I. ABADLIA, H. BOUZERIA, "PV-battery energy storage system operating of asynchronous motor driven by using fuzzy sliding mode control," international journal of hydrogen energy, Elsevier, pp. 1-9, 2016.

[BEN13] Y. BENDAHA, "Contribution à la commande avec et sans capteur mécanique d'un actionneur électrique," Thèse de Doctorat de l'université des sciences et de la technologie d'Oran, Algérie, Juillet 2013.

[**BEN15**] R. Benamara, Direct Torque Control Techniques for Induction Machines, Master's thesis, 2015.

[**KHI16**] Y. Khireddine, Sliding Mode Control of Asynchronous Motors, Master's thesis, 2016.

[**ALI17**] A. Ahmed, Field-Oriented Control of Dual-Star Induction Motors, Master's thesis, 2017.

[**HAM18**] S. Hamdi, Sensorless Control Algorithms for Asynchronous Machines: A Comparative Study, Master's thesis, 2018.

[**BOU19**] L. Bouzid, Fuzzy Logic Control of Double-Star Induction Machines, Master's thesis, 2019.

[AMM17] A. AMMAR, A. BOUREK, A. BENAKCHA, "Robust SVM-direct torque control of induction motor based on sliding mode controller and sliding mode observer," Frontiers in Energy, pp. 1-14, 2017.

[LAZ18] M. H. LAZREG, A. BENTAALLAH, "Sensorless fuzzy sliding-mode control of the double-star induction motor using a sliding-mode observer," ELEKTROTEHNIŠKI VESTNIK, vol. 85, no. 4, pp. 169-176, 2018.

[BEN18] M. H. LAZREG, A. BENTAALLAH, "Different Techniques for double star induction machine drive under GUI / Matlab," IEEE International Conference on Applied Smart Systems (ICASS'2018), Medea, Algeria, 24-25 November 2018.

[LAZ17] M. H. LAZREG, A. BENTAALLAH, "Field oriented control and sliding modecontrol of double star induction machine : comparative study," The 3rd International Conferenc e on Power Electronics and their Applications ICPEA, Djelfa, Algeria, 16-17 septembre 2017.

Annexe

Annexe

►D.1 - Paramètres de la machine asynchrone à double étoile :

Symbole of parameters	Numerical value
Rated Power P_n	4.5 KW
Ratedcurrent I_n	6.5 A
Rated voltage V_n	220/380 V
Ratedfrequency f_n	50Hz
Résistances statorique R_{s1}, R_{s2}	3.72 Ω
Résistance rotorique R_r	2.12 Ω
Inductance statorique L_{s1}, L_{s2}	0.022 H
Inductance rotorique L_r	0.006H
Inductance mutuelle L_m	0.3672 H
Coefficient de frottementfv	0,001 Nm s/rd
Tension du bus continu U_{DC}	1200V
Moment d'inertie J	0.0625 kg.m^2
Nombre de paires de pôles p	1